MICROCOPY   CHART

AFWAL-TR-85-2091

TECHNOLOGY DEVELOPMENT FOR SMALL HIGH SPEED,
MAINSHAFT ROLLER BEARINGS

W. K. CRAWFORD
P. F. BROWN

United Technologies
Pratt and Whitney Canada
Box 10
Longueuil, Quebec J4K 4X9

April 1986

Final Report for Period September 1978 - October 1985

DTIC
ELECTE
JUN 1 0 1986
S
D
D

Approved for public release; distribution unlimited

COPY

AFWAL-TR-85-2091

NOTICE

When Government drawings, specifications, or other data are used for any purpose other than in connection with a definitely related Government procurement operation, the United States Government thereby incurs no responsibility nor any obligation whatsoever; and the fact that the government may have formulated, furnished, or in any way supplied the said drawings, specifications, other data, is not be regarded by implication or otherwise as in any manner licensing the holder or any other person or corporation, or conveying any rights or permission to manufacture use, or sell any patented invention that may in any way be related thereto.
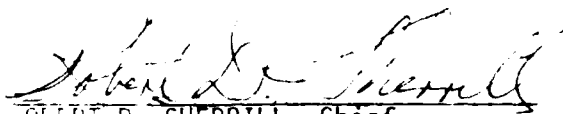
This report has been reviewed by the Office of Public Affairs (ASD/PA) and is releasable to the National Technical Information Service (NTIS). At NTIS, it will be available to the general public, including foreign nations.

This technical report has been reviewed and is approved for publication.

JOHN B. SCHRAND
Project Engineer
Lubrication Branch

HOWARD F. JONES, Chief
Lubrication Branch
Fuels & Lubrication Division

FOR THE COMMANDER

ROBERT D. SHERRILL, Chief
Fuels & and Lubrication Division
Aero Prepulsion Laboratory

"If your address has changed, if you wish to be removed from our mailing list, or if the addressee is no longer employed by your organization please notify AFWAL/POSL, W-PAFB OH 45433-6563, to help us maintain a current mailing list".

Copies of this report should not be returned unless return is required by security considerations, contractual obligations, or notice on a specific document.

HDA 118694

REPORT DOCUMENTATION PAGE

1a REPORT SECURITY CLASSIFICATION UNCLASSIFIED		1b RESTRICTIVE MARKINGS		
2a SECURITY CLASSIFICATION AUTHORITY		3 DISTRIBUTION/AVAILABILITY OF REPORT Approved for public release Distribution unlimited		
2b DECLASSIFICATION DOWNGRADING SCHEDULE				
4 PERFORMING ORGANIZATION REPORT NUMBER(S)		5 MONITORING ORGANIZATION REPORT NUMBER(S) AFWAL-TR-85-2091		
6a NAME OF PERFORMING ORGANIZATION United Technologies Pratt & Whitney Canada	6b. OFFICE SYMBOL (If applicable)	7a. NAME OF MONITORING ORGANIZATION Air Force Wright Aeronautical Laboratories Aero Propulsion Laboratory (AFWAL/POSL)		
6c ADDRESS (City. State and ZIP Code) Longueuil, Quebec J4K 4X9		7b. ADDRESS (City. State and ZIP Code) Wright-Patterson Air Force Base, Ohio, 45433		
8a NAME OF FUNDING/SPONSORING ORGANIZATION Aero Propulsion Laboratory	8b. OFFICE SYMBOL (If applicable) AFWAF/POSL	9 PROCUREMENT INSTRUMENT IDENTIFICATION NUMBER F33615-78-C-2049		

8c ADDRESS (City. State and ZIP Code) Wright-Patterson AFB, Ohio 45433	10 SOURCE OF FUNDING NOS			
	PROGRAM ELEMENT NO	PROJECT NO	TASK NO.	WORK UNIT NO
11 TITLE *Include Security Classification* Technology Development for Small High Speed, Mainshaft Bearings.	62203F	3048	06	97

12 PERSONAL AUTHOR(S)
W.K. Crawford/R. Kovacik, P.F. Brown

13a TYPE OF REPORT Final	13b TIME COVERED FROM __78910__ TO _851030_	14 DATE OF REPORT (Yr. Mo.. Day) April 1986	15. PAGE COUNT 118

16 SUPPLEMENTARY NOTATION
This was a cooperative program jointly funded by the U.S. Air Force, the Canadian
Government and P&WC.

17	COSATI CODES		18 SUBJECT TERMS *(Continue on reverse if necessary and identify by block number)*
FIELD	GROUP	SUB GR	Cylindrical Roller Bearings
21	05		Gas Turbine Mainshaft Roller Bearings
11	09		

19 ABSTRACT *(Continue on reverse if necessary and identify by block number)*

High speed experimental tests on small cylindrical roller bearings provided data on
parametric variables. The results were correlated with the analytical model developed
on NAPC contract N00140-76-C-0383.

20 DISTRIBUTION AVAILABILITY OF ABSTRACT UNCLASSIFIED UNLIMITED ☒ SAME AS RPT ☐ DTIC USERS ☐	21 ABSTRACT SECURITY CLASSIFICATION Unclassified	
22a NAME OF RESPONSIBLE INDIVIDUAL Schrand, John B	22b TELEPHONE NUMBER *Include Area Code* 513 225 7477	22c OFFICE SYMBOL AFWAL/POSL

DD FORM 1473, 83 APR   EDITION OF 1 JAN 73 IS OBSOLETE

FOREWORD

This report describes the work performed by the Pratt &
Whitney Canada Inc., of United Technologies Corporation,
Box 10, Longueuil, Quebec J4K 4X9 under U.S. Air Force
Contact No. F33615-78-C-2049 and Canadian Government (DRIE)
Contract Nos. CCC file No. 14SU.70C3-78-R-2049 and DDS file
No. 14ST.67023-8-0167. This is a final report covering work
conducted from 10 September 1978 to 30 October 1985.

John Schrand of the Air Force Wright Aeronautical
Laboratories, Aero Propulsion Laboratory, WPAFB (telephone
513-255-7477) provided the technical direction for the Air
Force portion of the program.

The project was conducted at Pratt & Whitney Canada Inc.,
under the direction of W.K. Crawford/C. Brownridge Program
Managers, R. Kovacik Principal Investigator, and Test
Engineers H. Powell, J. Crockett, G. Rutkowski, and
D. Koroyannakis. The efforts of J. Pennycook and
J. Spedaliere for typing of the text and J. Robshaw for
preparing the figures presented in this report are
gratefully acknowledged.

Appreciation is extended to the following Pratt & Whitney
Aircraft personnel of East Hartford who contributed to the
writing of this report, coordinated by P.F. Brown.

Robert A. Mattern, Jr., under the direction of
Frederick E. Dauser, Jr., conducted the statistical
analysis and Michael J. Carrano with John D. Robinson
evaluated the applicability of the statistical analysis
results. For correlation with TRIBO 1 Ming L. Shen reviewed
the wear model in the context of the 60 mm bearing test
program results.

Acknowledgement is also accorded the bearing manufacturing
companies that supplied the experimental hardware for this
program; FAG Bearings Corporation 8720 Schweinfurt, Germany
for the initial bearings (ESK 9244-01 to -11) and Split Ball
Bearing Division of MPB Corporation Lebanon, New Hampshire
for the additional test bearings (ESK 9785-01 to -04).

-iii-

TABLE OF CONTENTS

TABLE OF CONTENTS (CONT'D)

TABLE OF CONTENTS (CONT'D)

LIST OF ILLUSTRATIONS

LIST OF ILLUSTRATIONS (CONT'D)

LIST OF ILLUSTRATIONS (CONT'D)

LIST OF ILLUSTRATIONS (CONT'D)

LIST OF TABLES

1.0 INTRODUCTION

1.1 Background

The design and development of advanced aircraft turbine
engines with higher thrust to weight ratios and improved
efficiency in the form of increased thrust specific fuel
consumption is being achieved by an increase in rotor
speeds. In order to reduce overall engine weight and
minimize disruption in the gas path by the introduction of
struts and vanes, bearing supports have increasingly become
more flexible while shaft diameters have increased to pro-
vide high bending and torsional stiffness. These factors
have combined to generate bearings with increased dn numbers
(bearing bore in millimeters times shaft speed in
revolutions per minute) while allowing for greater unit
misalignment capabilities. As indicated in Figure 1, it is
anticipated that speed levels to 3.0 Mdn (million DN) will
be required by mid 1990s engine design.

The influence of geometric variations on roller
dynamics is increased at higher DN levels, and in many cases
it has been the performance of the roller bearing which has
compromised engine design. It is therefore imperative that
all aspects of roller bearing geometric design be analysed
as to their effect upon bearing performance. Field data
accumulated has indicated that bearing performance is very
sensitive to rolling element instabilities. This fact has
been exemplified in the

-1-
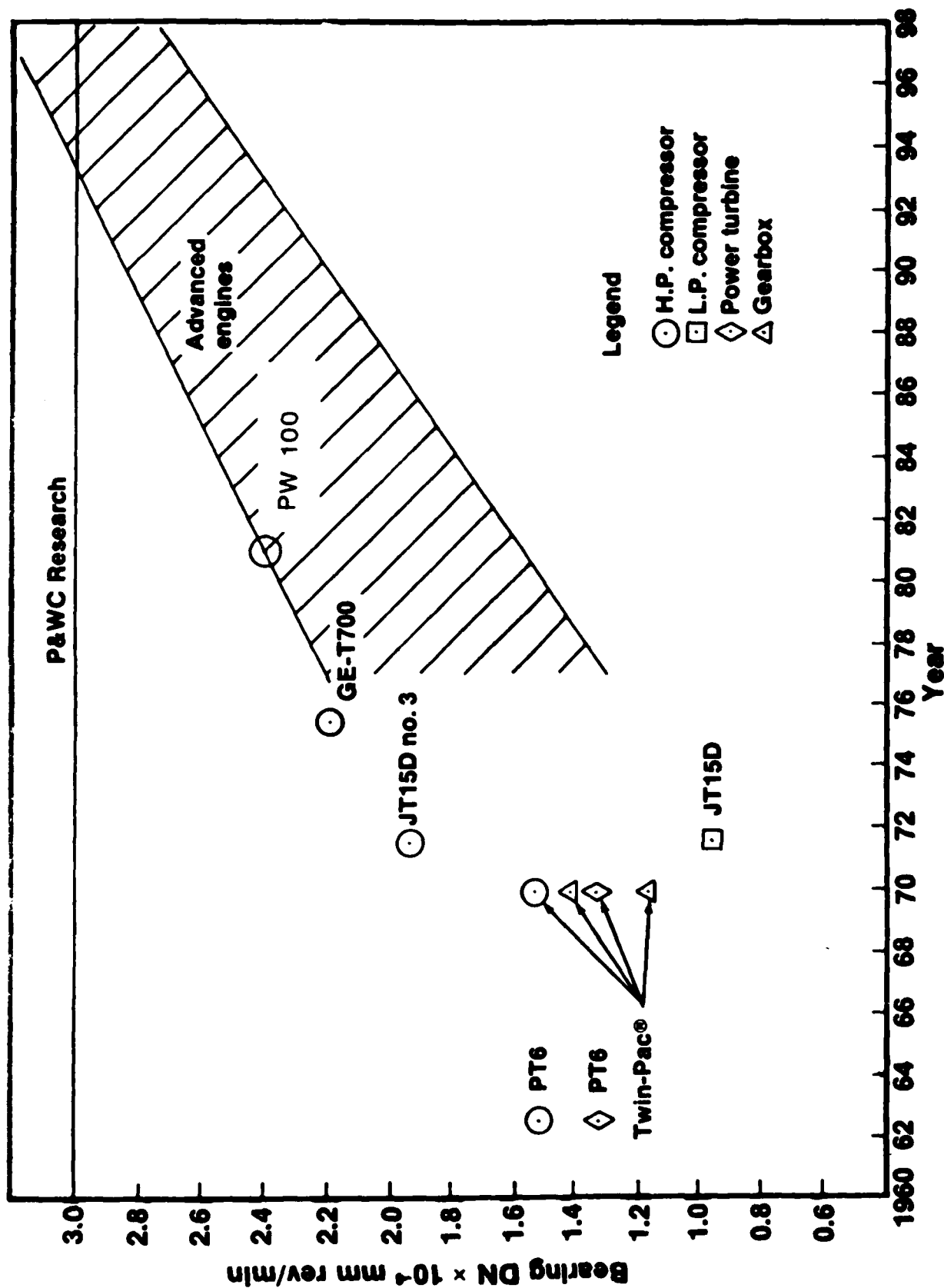
FIGURE 1   TREND TOWARDS INCREASED DN
VALUES FOR MAINSHAFT BEARINGS

-2-

occurrences of roller bearing cage fractures that have taken place in a turbofan engine compressor rotor system. The nature of this fracture is graphically presented in figure 2. These instabilities are exacerbated in high DN bearings and can cause roller skewing. This failure mode is precipitated by the rapid eccentric wear on the end surface of the rolling element or elements shown in figure 3.

Roller skidding by definition occurs when the rolling elements orbit the bearing at a speed below epicyclic. It is believed that skidding is associated with light radial loading at high shaft speeds. The resultant damage is limited to the contact surfaces. The mechanism for skid control is readily accessible in the application of increased bearing loading. This increase is most usually achieved by supplementing the bearing external load with an internal preload design.

There are, of course, numerous possible influences on rollers, most of which are inter-dependent to some extent as indicated in figure 4. Of these numerous parameters, the testing was restricted to those which were concluded by P&WA (see ref. 1) testing to be most significant.

An equally significant outcome of this testing was to be the correlation of 60 mm (bore) bearing data with that undertaken by P&WA in their bearing test program on 124 mm bearings (see ref. 1). There has been, to date, a necessary assumption that the influence of bearing geometric irregularities are of equal significance irrespective of

-3-
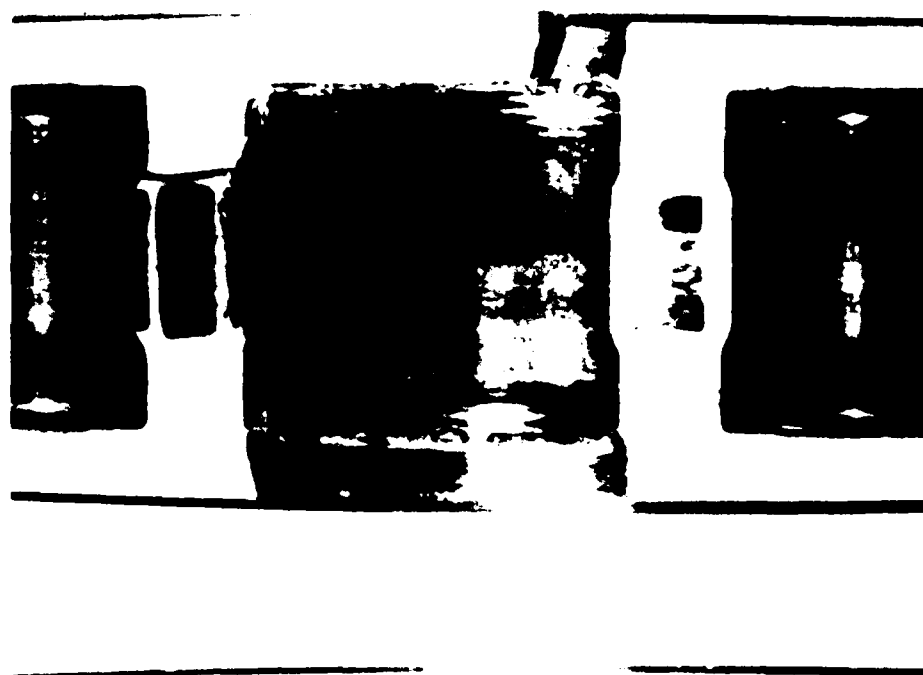
FIGURE 2   CAGE FRACTURE IN
TURBOFAN ENGINE

FIGURE 3   ROLLER ECCENTRIC
END WEAR
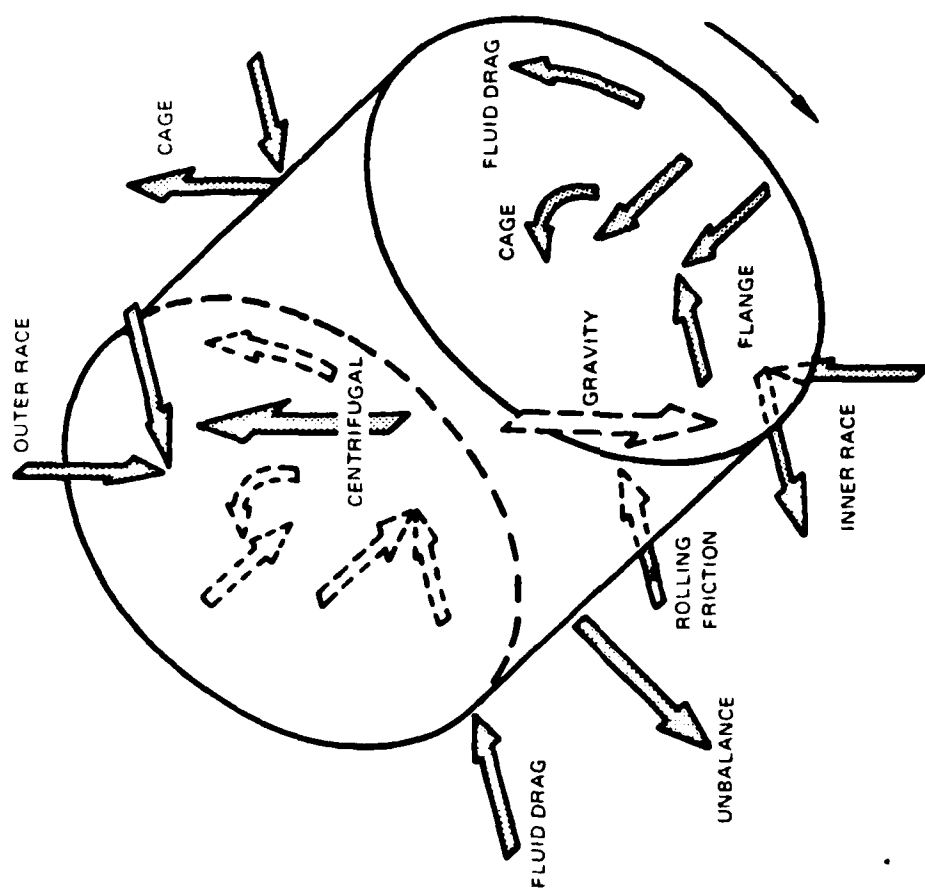
FIGURE 4   ROLLER FORCE AND MOMENT SYSTEM

Labels in figure: CAGE, OUTER RACE, CENTRIFUGAL, FLUID DRAG, UNBALANCE, ROLLING FRICTION, INNER RACE, FLANGE, GRAVITY, CAGE, FLUID DRAG

bearing size. The conclusions resulting from this test program could therefore facilitate the inclusion of a bearing scaling factor which would be incorporated within the bearing analysis programs currently being used.

In summary, therefore, the motivation for this study was the consistent increase in bearing DN values, and the associated influence of roller skewing and skidding upon bearing failure. Furthermore, there exists the need to establish the effect of bearing design and manufacturing runout tolerances.

2.0 EXPERIMENTAL PROGRAM DESCRIPTION

2.1 Objective

It is the primary objective of this program to investigate the phenomenon of eccentric roller end wear in small diameter (40 to 60 mm bore), high speed (up to 3.0 Mdn) roller bearings.

The program is designed to investigate the relative influence of a number of design and manufacturing variables on roller end wear to permit ranking of these variables in order of importance. It is further intended that the program provide information relating to the accuracy of extrapolation of conclusions (reached in an earlier program conducted by Pratt & Whitney Aircraft (Ref. 1)) from 124 mm bearings to 40-60 mm bearings. Should the findings show that small diameter bearings manifest different behaviour than do large bearings, it is a further objective to modify the computer analysis developed by PWA (TRIBO-1) and currently installed at Wright-Patterson AFB to provide the appropriate corrections to make it applicable to small diameter bearings.

Secondary objectives were to measure various roller bearing performance characteristics such as cage speed, heat generation, and efficiency of the lubricant delivery system.

2.2 Test Program Outline

The test program undertaken to attain the objective was composed of two major parts: a series of 10-hour tests on bearings manufactured with controlled levels of manufacturing and design variables at speeds up to 50,000 RPM (3.0 Mdn) and two 60-hour demonstration endurance tests on prototype bearings designed using knowledge gained from the first part of the program. The endurance tests were to be conducted on both 60 mm and 40 mm bore diameter bearings. The latter test was to demonstrate scalability of conclusions reached on the 60 mm tests to 40 mm. In an attempt to avoid bias in the ranking of variables, the test bearing set was designed using the partial factorial statistically designed experiment approach.

2.3 Design and Manufacturing Variables

Roller bearing parameters which are considered influential to skewing are presented in Table 1[1]. The basic categories considered were design geometries, manufacturing tolerances and quality control variables. Based on experience gained from the P&WA test program, it was decided that 7 parameters would be considered (See Table 2). It is apparent that six (6) of the seven (7) parameters included were chosen from category I. An additional parameter of guide flange designs based upon a curvature radius of 2.0 inches was introduced from category II. The parameter of roller length variation, although presented in category III,

[1] 1. REPRODUCED FROM REFERENCE 1.

TABLE 1 RELATIVE RANKING OF ROLLER BEARING VARIABLES

Roller Bearing Variable	Possible Effect of Variation	Rationale
CATEGORY I		
Roller Length Diameter Ratio	Uneven roller end wear	Alters roller element gyroscopic action stability achieved by L/D ratio of 0.8?
Roller tolerance (eccentricity, material, metered runout crown radii as run out)	Uneven roller end wear	Alters skewing forces as rollers impact guide flanges
Preload	Cage slewing and reduce damage or roller surfaces and raceway surfaces	Roller element skids or slips "out of gear" due to insufficient loading
Cage clearance	Local cage bore wear, inner land guided cage end wear, adjacent rollers and skidding damage	Rub causes local overheating and decreases effectiveness of oil film
Roller Flat Concentricity	Uneven roller end wear	Alters tractive force profile of roller as well as stability about transverse axis due to unsymmetrical roller mass distribution
Roller End Circular Runout	Uneven roller end wear	Affects roller stability about transverse axis and modifies roller end face contact stress
Roller End Shape	Uneven and concentric roller end wear	Alters lubrication film and roller end contact stresses
Raceway Taper	Concentric roller end wear	Alters distribution of roller tractive forces
Roller End Clearance	Uneven roller end wear	Alters maximum roller skewing angle thus changing end face contact forces
Roller Diameter Variation	Uneven and concentric roller end wear roller skid damage	Alters maximum roller skewing angle alters roller tractive forces
Lubrication	Uneven and concentric roller end wear roller skid damage	Alters effective oil film thickness
Flange Height	Uneven and concentric roller end wear	Alters roller skewing angle and roller end contact stress and luxation
Raceway Angular Misalignment	Concentric roller end wear reduced fatigue life	Alters roller tractive forces and distribution alters roller load profile
Roller tolerance (eccentricity ...)	Fatigue life and concentric roller end wear	Alters roller load profile tractive forces and skewing moment
CATEGORY II		
Roller tampering load	Concentric roller end wear	Reduction in roller end clearance due to guide flange deflection alters oil film thickness and roller end contact profile

---

TABLE 1 RELATIVE RANKING OF ROLLER BEARING VARIABLES (Continued)

Roller Bearing Variable	Possible Effect of Variation	Rationale
Flange Face Runout	Uneven roller end wear	Alters maximum roller skewing angle and dynamic end face loads
Roller Crown Radius	Fatigue life and concentric roller end wear	Alters roller load profile modifies tractive forces and skewing moments
Extended Roller Flat Length	Fatigue life and uniform end wear	Alters roller load profile tractive forces and skewing moment
Flange Face Waviness	Uneven roller end wear	Alters maximum roller skewing angle and dynamic end face loads
Flange Layback Angle	Uneven roller end wear concentric roller end wear	Alters maximum roller skewing angle oil film thickness and location of end face contact area
Roller Cage Pocket Clearance	Uneven roller end wear	Affects transmission of any cage in stability altering roller to guide flange contact loads and tractive forces
Flange Contour	Uneven roller end wear concentric roller end wear	Alters maximum roller skewing angle oil film thickness and roller end contact area and location
CATEGORY III		
Roller Length Variation	Uneven roller end wear	Alters maximum roller skewing angle
Cage Pocket Offset	Not apparent unless extreme causing uneven roller end wear	Alters resultant skewing force of roller element
Roller End Surface Finish	Uneven and concentric roller end wear	Alters oil film thickness requirements at roller ends
Flange Surface Finish	Uneven and concentric roller end wear	Alters oil film thickness requirements at roller ends
Raceway Surface Finish	Skid damage	Alters roller tractive forces and oil film thickness requirements at roller raceway contacts
Cage Pocket Squareness	Concentric roller end wear	Alters resultant skewing force acting on roller element
Raceway Waviness	Skid damage	Impacts dynamic loads on roller affecting variations in tractive force and oil film thickness requirements at contacts
Roller Taper	Uneven roller end wear	Alters tractive force profile of rollers as well as roller stability about transverse axis duct unenvironmental mass distribution

is included in the length to diameter ratio of category I
(since all rollers are standardized at .2756 in (7 mm)).

The relative magnitude of the original test bearing
parameters proposed is presented in Figure 5A. The actual
relative values of parameters peculiar to each bearing which
was to be tested are presented in the matrix of figure 5B.
Test bearings prefixed by ESK 9785 were additional bearings
which would be required to separate the test parameters of
"roller end circular runout", "corner radius runout" and
"roller crown drop runout". That is, as a result of
manufacturing limitations, the original bearings (prefixed
by ESK 9244) did not adequately differentiate these
parameters with respect to the tolerance ranges. In
addition, continued difficulties in producing a roller with
a high "roller crown drop runout" necessitated the removal
of this parameter from the test list.

The combinations of the variables among the test bearings is
indicated by two levels of parameter variation and are
represented by "H" (High) and "L" (Low) respectively, with
the horizontal axis representing bearing design
consideration while the vertical axis represents
manufacturing tolerance controls.

2.3.1 Test Bearing Table 2a represents the original
tolerance requirements. The values used with this table
have been established by analytical designs and

FIGURE 5A: 3.0 MDN PROGRAM
TEST MATRIX (ORIGINAL)

FIGURE 5B: 3.0 MDN PROGRAM TEST MATRIX (MODIFIED)

manufacturing or production experience. In the case of a particular parameter which was not to be considered within any test bearing, that parameter value was kept at the level of the baseline bearing, i.e., ESK 9244-11. The actual levels of bearing parameters referenced in figure 5B are presented in table 2B with the unshaded boxes highlighting the deviations.

2.4 Bearing Configuration

2.4.1 Geometric Representation At the conceptual stage of this program, it was decided that the bearing configuration chosen should not only compliment the P&WA work on 124 mm bearings, but should reflect the design and operating environment peculiar to small engines.

The bearing size selected for the test program was based upon a bearing located on the compressor rotor of a modern turbofan engine.

2.4.2 Bearing General Description The basic roller bearing selected for the test program is shown in Figure 6. The bearing is a 24 roller, under-race lubricated bearing with a 60 mm bore diameter. The initial bearings prefixed by ESK 9244 were manufactured by "FAG" of Schweinfurt Germany, from M-50 (AMS 6490) steel in accordance with (Canadian Pratt & Whitney company specification) CPW 378 Specifications. The additional bearings (prefixed by ESK 9785) were manufactured by "Split Ball Bearing" of Lebanon, New Hampshire. For the purpose of this test

TABLE 2a   3 MDN PROGRAM-SPECIFIED TEST BEARING DIMENSIONS

CUSTOMER PART NO.	CORNER RAD. RUNOUT (in)	(mm)	END SQUARE RUNOUT (in)	(mm)	CROWN DROP RUNOUT (in)	(mm)	ROLLER LENGTH (in)	(mm)	ROLLER END CLEARANCE (in)	(mm)	INNER RING RACEWAY TAPER	LAND RIM DIA. MIN. in (mm)	GUIDE FLANGE STYLE
ESK 9244-01	.0002 max.	0.005 max.	.00006 max.	.0015 max.	.0020 .0015	0.051 0.038	.3150	8	.0016 .0008	0.040 0.020	0.75' max.	2.698 (68.53)	2
ESK 9244-02	.0002 max.	0.005 max.	.0002 min.	0.005 min.	.0001 max.	.0025 max.	.3150	8	.0016 .0008	0.040 0.020	4.50' 3.25'	2.698 (68.53)	1
ESK 9244-03	.0002 max.	0.005 max.	.0002 min.	0.005 min.	.0020 .0015	0.051 0.038	.2362	6	.0016 .0008	0.040 0.020	0.75' max.	2.753 (69.93)	1
ESK 9244-04	.0002 max.	0.005 max.	.0002 min.	0.005 min.	.0020 .0015	0.0512 0.038	.3150	8	.0016 .0008	0.040 0.020	0.75' max.	2.698 (68.53)	1
ESK 9244-05	.0002 max.	0.005 max.	.00006 max.	.0015 max.	.0001 max.	0.0025 max.	.2362	6	.0035 .0027	0.089 0.069	4.50' 3.25'	2.753 (69.93)	2
ESK 9244-06	.0015 min.	0.038 min.	.00006 max.	.0015 max.	.0001 max.	0.0025 max.	.2362	6	.0016 .0008	0.040 0.020	0.75' max.	2.698 (68.53)	1
ESK 9244-07	.0015 min.	0.038 min.	.0002 min.	0.005 min.	.0020 .0015	0.051 0.038	.3150	8	.0016 .0008	0.040 0.020	4.50' 3.25'	2.753 (69.93)	2
ESK 9244-08	.0015 min.	0.038 min.	.0002 min.	0.005 min.	.0020 .0015	0.051 0.038	.2362	6	.0035 .0027	0.089 0.069	4.50' 3.25'	2.698 (68.53)	2
ESK 9244-09	.0015 min.	0.038 min.	.0002 min.	0.005 min.	.0001 max.	0.0025 max.	.3150	8	.0035 .0027	0.089 0.069	0.75' max.	2.753 (69.93)	2
ESK 9244-10	.0015 min.	0.038 min.	.00006 max.	.0015 max.	.0020 .0015	0.0512 0.038	.3150	8	.0035 .0027	0.089 0.069	4.50' 3.25'	2.753 (69.93)	1
ESK 9244-11	.0002 max.	0.005 max.	.0001 max.	.0025 max.	.0001 max.	0.0025 max.	.3150	8	.0016 .0008	0.040 0.020	0.75' max.	2.720 (69.09)	1

GUIDE FLANGE STYLE
1/ TAPERED 15'- 40'
2/ RADIUSED 2.00IN R.

TABLE 2b   3   MDN PROGRAM-SUPPLIED TEST BEARING DIMENSIONS

TEST BEARING PART NO.	CORNER RAD. RUNOUT in	mm	END SQUARE RUNOUT in	mm	CROWN DROP RUNOUT in	mm	ROLLER LENGTH in	mm	ROLLER END CLEARANCE in	mm	INNER RING RACEWAY TAPER	LAND RIM DIA. MIN. in (mm)	GUIDE FLANGE STYLE
ESK 9244-01	.0002 max.	0.005 max.	.00006 max.	.0015 max.	.00006 max.	.00152 max.	.3150	8	.0016 .0008	0.040 0.020	0.75° max.	2.698 (68.53)	2
ESK 9244-02	.0002 max.	0.005 max.	.0001 max.	.0025 max.	.0001 max.	.0025 max.	.3150	8	.0016 .0008	0.040 0.020	4.50° 3.25°	2.698 (68.53)	1
ESK 9244-03	.0002 max.	0.005 max.	.0001 max.	.0025 max.	.00004 max.	.00102 max.	.2362	6	.0016 .0008	0.040 0.020	0.75° max.	2.753 (69.93)	1
ESK 9244-04	.0002 max.	0.005 max.	.0001 max.	.0025 max.	.00004 max.	.00102 max.	.3150	8	.0035 .0027	0.089 0.069	0.75° max.	2.698 (68.53)	2
ESK 9244-05	.0002 max.	0.005 max.	.00006 max.	.0015 max.	.0001 max.	0.0025 max.	.2362	6	.0035 .0027	0.089 0.069	4.50° 3.25°	2.753 (69.93)	1
ESK 9244-06	.0015 min.	0.038 min.	.0002 max.	.0051 max.	.0001 max.	0.0025 max.	.2362	6	.0016 .0008	0.040 0.020	0.75° max.	2.698 (68.53)	1
ESK 9244-07	.0015 min.	0.038 min.	.0002 min.	0.005 min.	.00006 max.	.00153 max.	.3150	8	.0016 .0008	0.040 0.020	4.50° 3.25°	2.753 (69.93)	2
ESK 9244-08	.0015 min.	0.038 min.	.0002 min.	0.005 min.	.00008 max.	.00203 max.	.2362	6	.0035 .0027	0.089 0.069	4.50° 3.25°	2.698 (68.53)	2
ESK 9244-09	.0015 min.	0.038 min.	.0002 min.	0.005 min.	.0001 max.	0.0025 max.	.3150	8	.0035 .0027	0.089 0.069	0.75° max.	2.753 (69.93)	2
ESK 9244-10	.0015 min.	0.038 min.	.0002 max.	.0051 max.	.00006 max.	.00152 max.	.3150	8	.0035 .0027	0.089 0.069	4.50° 3.25°	2.753 (69.93)	1
ESK 9244-11	.0002 max.	0.005 max.	.0001 max.	.0025 max.	.0001 max.	0.0025 max.	.3150	8	.0016 .0008	0.040 0.020	0.75° max.	2.720 (69.09)	1
ESK 9785-01	.0015 min.	0.038 min.	.00006 min.	.0015 min.	***	***	.3150	8	.0035 .0027	0.089 0.069	0.75° max.	2.698 (68.53)	2
ESK 9785-02	.0002 max.	0.005 max.	.0002 min.	0.005 min.	***	***	.2362	6	.0035 .0027	0.089 0.069	0.75° max.	2.753 (69.93)	2
ESK 9785-03	.0015 min.	0.038 min.	.00006 min.	.0015 min.	***	***	.2362	6	.0016 .0008	0.040 0.020	4.50° 3.25°	2.698 (68.53)	1
ESK 9785-04	.0015 min.	0.038 min.	.0002 min.	0.005 min.	***	***	.2362	6	.0016 .0008	0.040 0.020	0.75° max.	2.698 (68.53)	1

GUIDE FLANGE STYLE
1/ TAPERED 15' - 40'
2/ RADIUSED 2.00IN R.

FIGURE 6   TEST BEARING
60mm BORE

program, a total of 17 bearings were manufactured. The
bearing inner ring provides for under race lubrication by 12
under race oil slots leading to radial oil holes supplying
equally the ring raceway as well as the cage land
diameters. The bearing outer ring is of a flanged design
provided with four clearance bolt mounting holes. A total
of 24 rollers were used to compliment a bearing set. Each
roller was identified on one end face by a number from 1 to
24 and were located in a sequential order within the cage
pockets. The cage was constructed without the roller
retention lugs in order to facilitate inspection of
individual rollers. In all other respects, the bearing cage
is similar to any standard inner land riding retainer
employed within P&WC.

2.5 Test Rig

2.5.1 Test Section The rig test section is shown in
figure 7a and is essentially separated into two major
compartments; the slave bearing section and the test bearing
section. The test bearing section is further subdivided
into the other compartments; one to receive oil that is
spilled or rejected at the test bearing axial scoops and the
other compartment receiving oil which has passed through the
test bearing. A flexible diaphragm issued to isolate
interaction with the drive system and the shaft is supported
by two bearings, one of which is the test bearing. Radial
loading is applied through a double set of roller bearings
while the shaft axial location as well as radial load
reaction is accomplished with a Conrad bearing. During
initial rig operation, reliability problems developed with

-18-

FIGURE 7a   TEST SECTION

PISTON
LOAD CYLINDER

RADIAL ACCELEROMETER

TEST BRG

UNDER RACE
OIL JET _ TEST BRG

CAGE SPEED
FIBRE OPTICS

T/C

OIL OUTLET
SCOOP REJECT

ROLLER SPIN
COIL (2 off)

OIL OUTLET
SCOOP PASSED

LOAD ARM

RADIAL
ACCELEROMETER

LOAD BRG
(2 off)

60 MIN
TEST SHAFT

T/C

T/C

SIDE JET
LOAD BRG

OIL OUTLET
SCOOP PASSED

SIDE OIL JET
SUPPORT BRG

SUPPORT
BRG
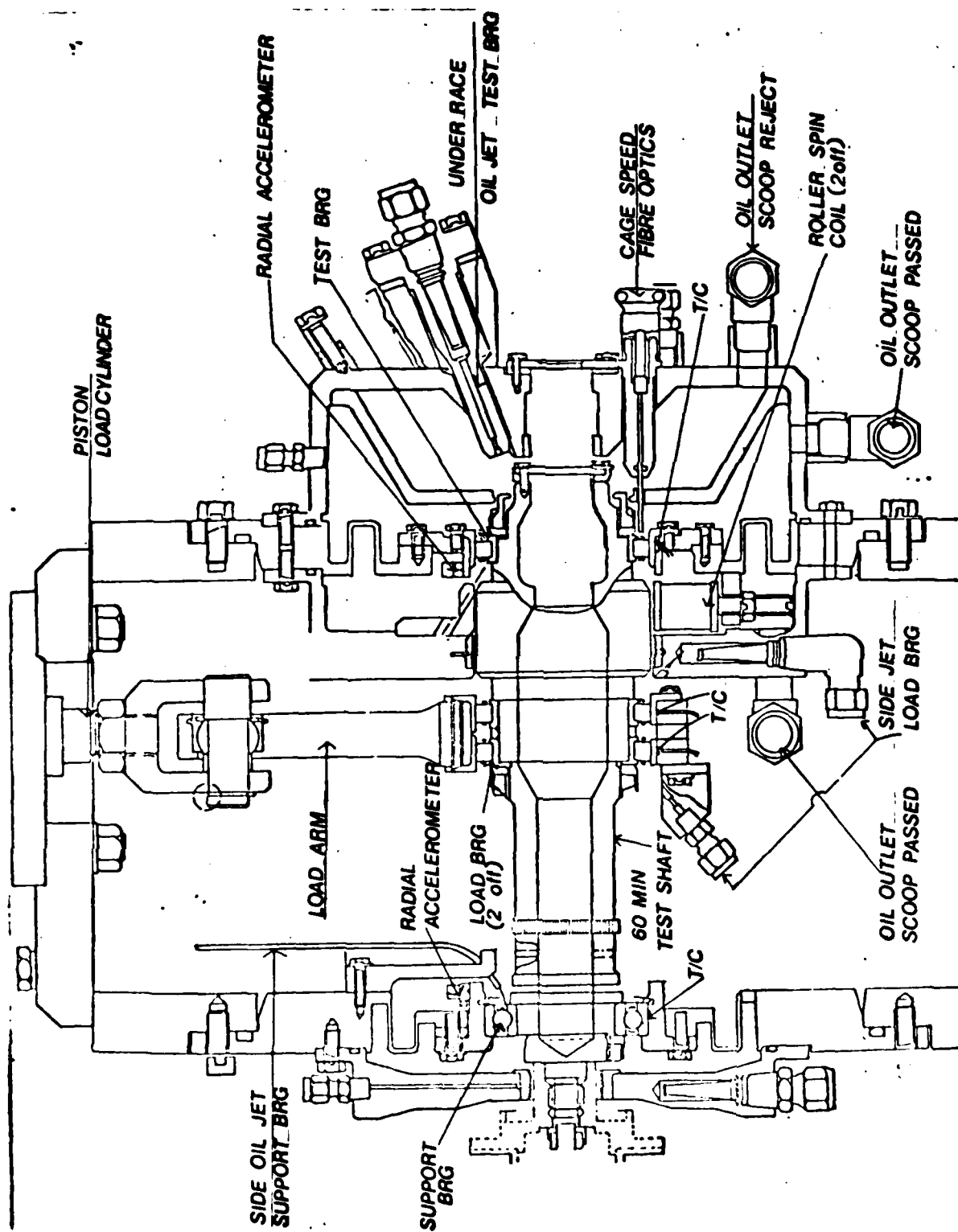
the load bearing, which required redesign action. Figure 7b
depicts the modifications made to the test section shaft to
provide increased stability to the load bearings, as well as
the introduction of under race lubrication to the load
bearings.

Note that prior to the modifications to the test
section shaft, as shown in figure 7b, the test bearing
radial loads were 100 lb, 300 lb and 500 lb rather than 85
lb, 250 lb and 400 lb respectively (see table 5). The
revised loadings were introduced (after testing of ESK
9244-11) to maintain the radial load at the Conrad ball
bearing to pre-test section shaft modification levels.

2.5.2 Drive Section The test section was driven
through a flexible diaphragm coupling manufactured by Bendix
and was used to isolate any possibility of bearing loading
which could have been introduced to the test section by
misalignment with the drive system. The power was supplied
by a 300 hp AC electric motor (Canadian General Electric
Model No. 142962) operating at the design speed of 3,560
rpm. The test section maximum operating speed of 50,000 rpm
was achieved through two General Electric speed increase
gear boxes (S231-X Low Speed, S231-AZ-1 high speed). The
speed control was by an eddy current coupling (Dynamic Corp.
Model No. WCS 216B), connected to the electric motor, the
maximum speed rating of the coupling is 3,600 rpm. The test
section and drive are schematically represented in Figure
7c.

2.5.3 Lubrication System Load bearing lubrication was
initially achieved by side jetting, however as the test
program proceeded, it became apparent that an under race oil
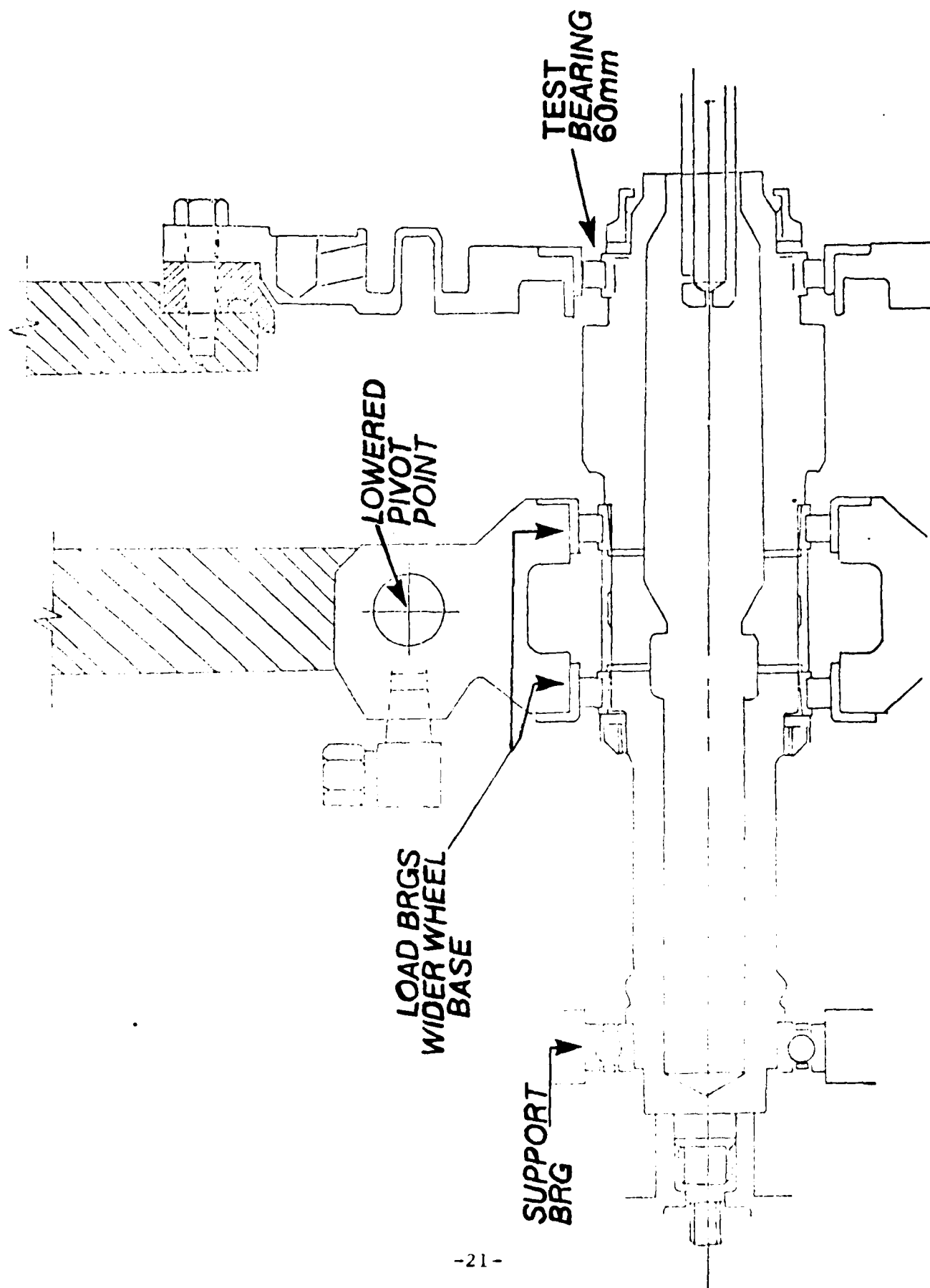
FIGURE 7b   TEST SECTION SHAFT MODIFICATION (TO PROVIDE UNDER RACE LUBRICATION TO LOAD BEARING)

-21-

ELECTRIC MOTOR

DYNAMATIC COUPLING

HIGH SPEED GEAR BOX

LOW SPEED GEAR BOX
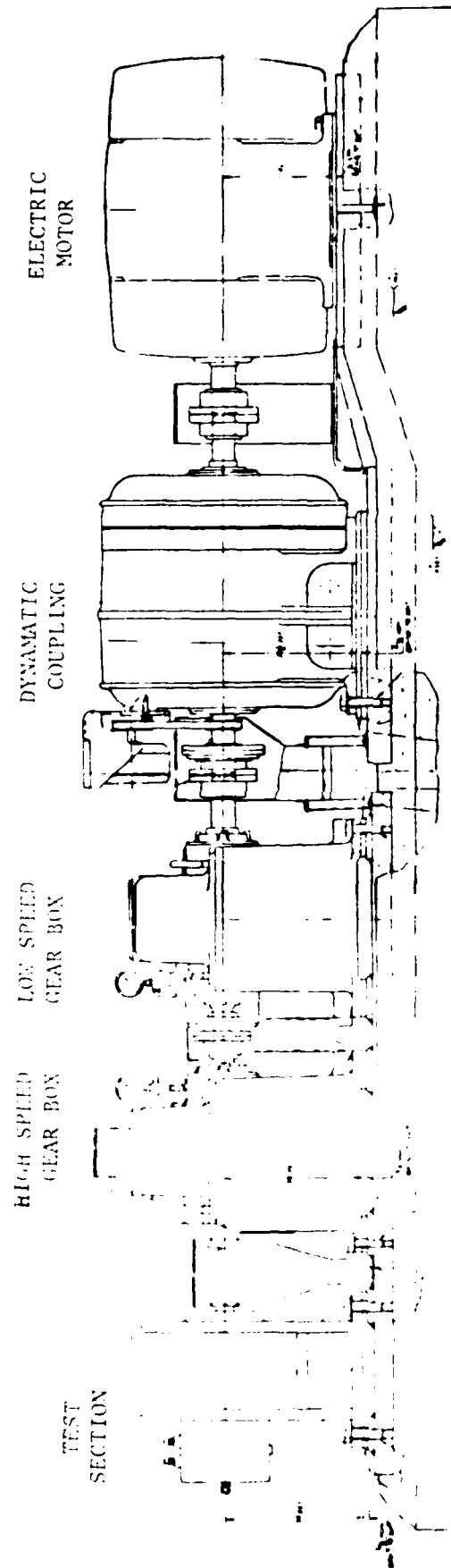
TEST SECTION

FIGURE 7c   TEST AND DRIVE SECTION ASSEMBLY

scheme would be required to control inner race temperatures. The final lubrication configuration, in schematic form, is shown in figure 8. In this design, it was possible to continually control the flowrates to the test and load bearings. The oil was introduced to the load bearings through the shaft bore (see figure 7b) while the test bearing lubrication was by an axial oil scoop. The lubrication to the ball bearing by side jetting was maintained. The test bearing compartment was segregated from the remainder of the test section. This compartment was divided further to separate the oil flows that passed through the test bearing to that rejected or spilled at the axial oil scoop. The electrical oil pump system was backed up by a pneumatic system which would be automatically initiated in the event of a failure in the primary lubrication system.

2.5.4 Instrumentation The instrumentation employed to monitor the bearing test was separated into two categories, one set was to record the performance of the test section which was subdivided into the test bearing and slave bearing operational conditions. The other set of instrumentation was to monitor the performance of the test section drive assembly parameters. Temperature measurements were made using Type T (copper/constantan) thermocouples while accelerometer readings were made with B+K accelerometers. All pressures were recorded on bourdon type gauges.
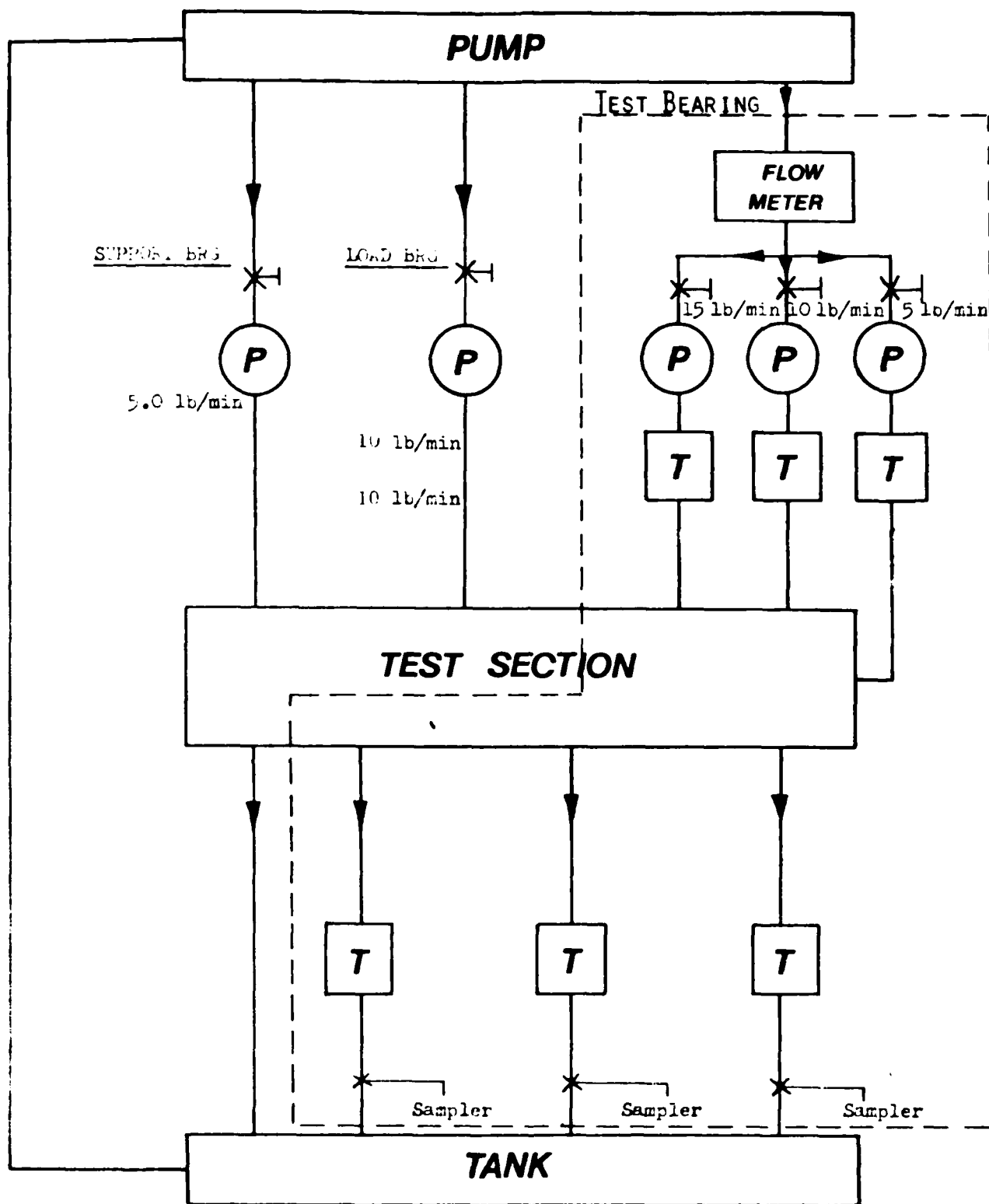
P = PRESSURE GAUGE

T = THERMOCOUPLE

ALL FLOWS AT 80 PSI

FIGURE 8   LUBRICATION SCHEMATIC

The test drive parameters consisted of temperature measurements at the eddy current coupling cooling water exit. Another set of thermocouples were used to measure the temperature of the bearing pads in the output of the high speed gearbox. Additional thermocouples and pressure gauges recorded temperatures and pressures of the drive system lubricant. The test section drive speed was monitored at the output of the high speed gearbox while circuit breakers provided additional safeguards for the electric motor and eddy current coupling.

In the case of the test section, all of the bearing outer raceway temperatures were measured at two azimuth locations. Initial attempts to record inner ring temperatures at the test roller bearing were abandoned when the telemetry system employed proved unreliable. With the introduction of under race lubrication at the load bearings through the bore of the shaft, (required for improved bearing reliability) measurement of inner ring temperatures by a slip ring also became impractical. The oil tank temperature was monitored as was the oil temperature at the jets to the test bearing. Oil scavenge temperature for both the oil passing through the test bearing and the oil rejected at the oil scoop were measured. A chip detector was located in the oil scavenge lines for both the test bearing oil scavenge and the oil returning from the load and support bearings.

B&K Accelerometers were installed in the test section
structure to detect radial accelerations at the test bearing
housing in both the horizontal and vertical directions. In
the loading arm an axial accelerometer was included in
addition to the radial gauges in the horizontal and vertical
directions.

The test bearing radial load was applied by reacting
the force applied at the load bearings by means of the pneu-
matic piston. Control was by the adjustment of a pressure
regulating valve to control the air pressure. The test
shaft rotational speed was measured by utilizing a Bentley
proximity probe to record the passing frequency of a toothed
wheel on the high speed gearbox output shaft. Oil
temperature was maintained by a Johnsons controller
regulating the flow of oil through the heat exchanger. Oil
heating was by five electric heaters (Chromolox 3 Kw)
installed in the oil tank.

Initially, all of the above parameters were monitored
manually. However after the first test run it became app-
arent that a form of automatic data recording (ADR) would be
required. It was also decided that limit values on the
parameters monitored must be included. These would provide
automatic rig shutdown should any of the preset limits on a
specified parameter be exceeded. The automatic data
recording system installed was an "Autodata Eight" with 36
channels programmed to monitor the test bearing functions of

-26-

speed, outer race temperatures as well as oil inlet and outlet temperatures. The remaining channels were used to monitor additional functions concerned with the performance of the drive system. The channels and associated shutdown limits are presented in Table 3 along with their assigned functions.

In addition to the ADR unit, an eight-channel tape recorder was employed during the testing (see Table 4 for channel definition). The tape recorder was an SE LAB model with a frequency response limit of 10 Khz and was therefore capable of recording any of the frequencies which were associated with the bearing performance. Indeed, the highest frequencies which would be encountered were those of roller spin speed and with a theoretical frequency of approximately 3 Khz the signal was well within the range of the unit employed. The test bearing cage speed was measured using fibre optics. In this arrangement, the end face of the cage was tarnished black, using a sodium sulfide solution, over 180 degrees of the circumference as shown in Figure 9. The optically contrasting surface was transformed into an electrical output which produced a square wave signal. By reducing the data onto a time function output, the cage rotational frequency could be established. The roller spin speed was obtained by magnetizing one roller element across its diameter so that each end face contained both a north and south pole, as is shown in Figure 10. Two coils mounted on the rig 180 degrees apart but adjacent to

-27-

TABLE 3
ADR HOOK-UP

ADR CHANNEL	LIMIT	PARAMETER	UNIT
000	275	Scoop Oil Inlet Temp.	°F
001	350	Scoop Oil Reject Temp.	°F
004	350	Oil Outlet, Test Rear	°F
005	350	Oil Outlet, Test Front	°F
006	350	Oil Outlet Supp. Brg.	°F
007	275	Oil Inlet Test Pump	°F
010	350	Test Brg. Outer Race T1	°F
011	350	Test Brg. Outer Race T2	°F
012	340	Load Brg. Left #1	°F
013	340	Load Brg. Left #2	°F
014	340	Load Brg. Right #1	°F
015	340	Load Brg. Right #2	°F
016	320	Supp. Brg. #1	°F
017	320	Supp. Brg. #2	°F
018	240	H/S Pinion #1 Skin Temp. Front Brg.	°F
019	240	H/S pinion #2 Skin Temp. Front Brg.	°F
020	240	H/S Pinion #3 Skin Temp. Front Brg.	°F
021	240	H/S Pinion #4 Skin Temp. Front Brg.	°F
022	240	H/S Pinion #1 Skin Temp. Back Brg.	°F
023	240	H/S Pinion #2 Skin Temp. Back Brg.	°F
024	240	H/S Pinion #3 Skin Temp. Back Brg.	°F

TABLE 3

ADR HOOK-UP (Concluded)

ADR CHANNEL	LIMIT	PARAMETER	UNIT
025	240	H/S Pinion #4 Skin Temp. Back Brg.	°F
026	350	H/S Gearbox Brg. #1	°F
027	350	H/S Gearbox Brg. #2	°F
028	350	H/S Gearbox Brg. #3	°F
029	350	H/S Gearbox Brg. #4	°F
040	425	Test Brg. Vert. (Left)	°F
041	425	Test Brg. Horiz. (Right)	°F
042	340	Load Brg. Vert.	°F
043	200	Load Brg. Horiz.	°F
044	200	Load Brg. Axial	°F
045	200	Supp. Brg.	°F
049	10V	Load Brg. Oil Flow	#/min
050	10V	Shaft Speed	rpm
051	0-110	Test Brg. Oil Pressure	psig
052	0-100	Load Brg. Oil Pressure	psig

TABLE 4

TAPE RECORDER HOOK-UP

CHANNEL	LIMIT	FUNCTION
1	10 KHz	a) To be used for load bearing roller passing frequency with ability to switch from load brg. A to B.
		b) To be able to superimpose voice on this channel.
2	1 KHz	To be used for shaft speed recording.
3	1 KHz	To be used for fibre optics recording on test bearing.
4	5 KHz	To be used for roller spin recording on test bearing.
5	10 KHz 450g OA (AA)	To be used for accelerometer at test bearing 1 off radial.
6	10 KHz 350g OA (AA)	To be used for accelerometer at load bearing 1 off radial.
7	10 KHz 200g OA (AA)	To be used for accelerometer at load bearing 1 off axial.
8	10 KHz 200g OA (AA)	To be used for accelerometer at support bearing 1 off radial.

SEE NOTE 2

POCKET No.1

ROLLER NUMBERED 1 TO 24
IN A CLOCKWISE DIRECTION
WHEN VIEWED FROM THIS SIDE
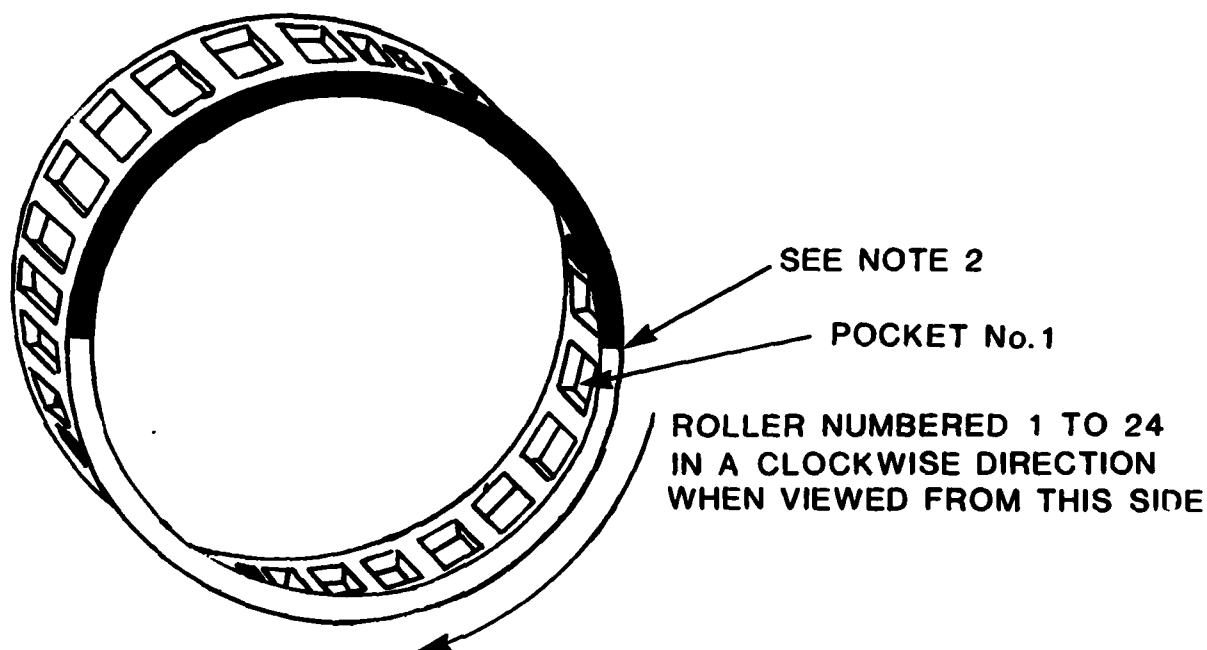
REFERENCE ROLLER BEARING ESK 9244

NOTE

1. 10% SODIUM SULFIDE TREATMENT TO CAGE SIDE RAIL ONLY
    i.e. CAGE POCKET, INNER CIRCUMFERENCE, AND OUTER
    CIRUMFERENCE TO BE FREE OF SILVER SULFIDE

2. SILVER SULFIDE TO STOP AT CROSS RAIL NEAREST LAST
    ALPHA-NUMERIC CHARACTER OF CAGE SERIAL NUMBER

3. TO BE APPLIED ON S/N SIDE OF CAGE

FIGURE 9   CAGE CONTRAST FOR FIBRE OPTICS

CAGE
SIDERAIL

N

S
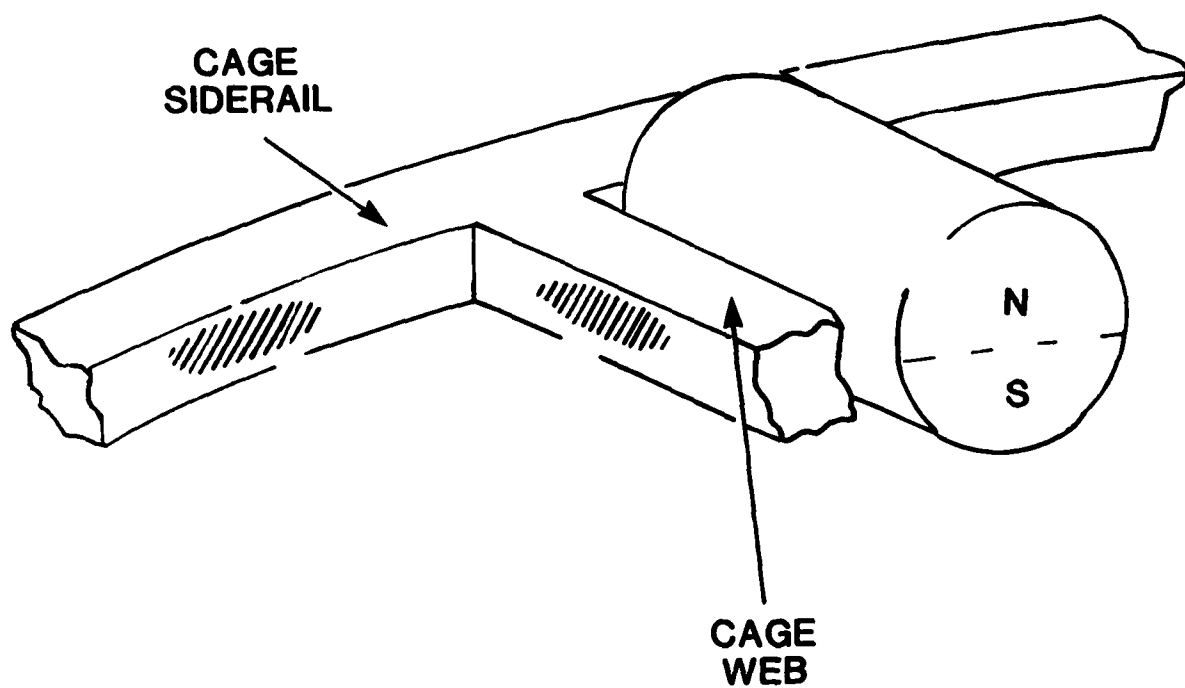
CAGE
WEB

FIGURE 10   ROLLER MAGNETIZATION

the shaft, would respond to the alternating north, south field produced as the roller rotated about its own axis. This roller was placed in the cage pocket adjacent to the location of the change in contrast on the cage end face. This position in the cage along with the orientation of the fibre optics probe in relation to the radial loading directions on the bearing would permit correlation of the roller azimuth position. By simultaneously triggering the cage and roller signal on a time trace output, the frequency of the roller spin about its own axis at any azimuth position could be established. This would permit correlation between roller spin speed and the azimuth location in relation to the radial load zone to be established.

2.6 TEST PROCEDURE

The test was conducted according to the schedule shown in Table 5, with a total duration of 10 hours per bearing. The test sequence consisted of three major components: initial calibration, steady state endurance operation and cyclic endurance.

The calibration run was conducted over the rotor speed range of 16,666 rpm to 50,000 rpm which corresponds to DN values from 1 MDN to 3 MDN (for the 60 mm test bearing employed). The schedule was further refined to evaluate three oil jet flow rates; the first being at 10 lb/min,

-33-

TABLE 5

TEST SCHEDULE

OIL SUPPLY		LOAD		PSIG	BEARING SPEED (rpm) / BEARING DN/TEST POINT NO.						TEST HOURS
UNDER RACE lb/min	TEMP deg. f	TEST BRG	REF LOAD BRG		16666 / 1.0	33333 / 2.0	41666 / 2.5	45933 / 2.75	48333 / 2.9	50000 / 3.0	
10	225	85	150	8.0	1	4	7	10	13	16	3
		250	443	23.5	2	5	8	11	14	17	
		400	710	8.0	3	6	9	12	15	18	
5	225	85	15	8.0	19	20	21	22	23	24	1
15	250	85	150	8.0	25	26	27	28	29	30	1
10	225	85	150	8.0	endurancement at 3M dn						4
10	225	85	150	8.0	2.0 ------------------> 2.75M dn <------------ dn accels =========== decels						1

* not including typical rotor unbalance of 0.015 oz-in which generates 66 lb at 3.0M dn

which included three radial loadings of 85 lb, 250 lb and 400 lb at the test bearing. The remaining two oil jet flows of 5 lb/min and 15 lb/min complimented only the one bearing loading of 85 lb. This entire calibration schedule comprised 30 individual test points of 10 minutes each. At the end of each individual test point, the pertinent parameters of bearing outer raceway temperatures, oil inlet and outlet temperatures were recorded. Oil flow rates through the oil scoop were measured during the speed steps for each of the oil jet flow rates.

Steady state bearing operation was conducted at a rotor speed of 50,000 rpm corresponding to 3 MDN. The test bearing radial load of 85 lb was also maintained constant throughout this 4-hour operation sequence as was the oil jet flow rate of 10 lb/min. The bearing parameters were recorded every half hour.

These points were only used to monitor the condition of the bearing as a safety measure to confirm its integrity throughout this sequence of the test schedule.

Cyclic rotor speeds from 33,333 rpm to 45,833 rpm provided the final stage in the test schedule. This cyclic endurance consisted of 1 hour of operation with each cycle from 2 MDN to 2.75 MDN and back to 2 MDN taking approximately 3 minutes. The oil jet flow rate was maintained at 10 lb/min and the test bearing radial loading remained constant at 85 lb. The bearing performance was monitored every quarter hour to establish the integrity of the bearing.

The bearings were tested according to the following randomly-selected sequence.

TEST BEARING	TEST COMPLETION DATE
ESK 9244-11	23/12/80
ESK 9244-03	15/04/82
ESK 9244-10	10/09/82
ESK 9244-09	28/09/82
ESK 9244-09A	21/10/82
ESK 9244-07	22/12/82
ESK 9244-02,	
ESK 9244-01,	
ESK 9244-08,	
ESK 9244-06,	
ESK 9244-09B,	
ESK 9244-04,	
ESK 9785-01,	
ESK 9785-02,	
ESK 9785-03,	
ESK 9785-04	

Test bearing 09 and 09A and 09B, were repetitions of the same predominant parameters. The consistency of the wear measurements from these three bearings would ensure that the testing procedure was not being altered.

The lubricant used for the test section was formulated according to MIL-L-7808. The initial quantity of oil was supplied by the USAF. However as testing proceeded, additional MIL-L-7808 oil was obtained from EXXON OIL.

2.7 Measurements

Prior to initiating the test schedule, each individual roller, which was numbered on the end face, was measured for roller skew angle, roller weight as well as roller dynamic unbalance.

2.7.1 Roller Geometric Measurements and Unbalance

Roller skew angles were obtained utilizing the fixtures shown in Figure 11. The individual roller was locked within the fixture using a thumb screw. The unit was then adjusted so that it was tangent with the bearing raceway at the point of roller contact with the inner raceway. The total side to side skewing motion of the roller and fixtures were measured at a known point from the roller axis. The skew angle therefore is the arc sine of one half of the total side-to-side skewing travel of the fixture.

The roller individual weights were measured using a Gramatic scale manufactured by Fisher Scientific Company. The actual model used was the Macro Gramatic catalog No. 1-910 with a capacity to 200 g. The specific performance data of this unit is a precision of ±.03 mg with an accuracy in the optical range of ±.05 mg.

The roller dynamic unbalance was obtained using a FAG balancing machine model MGR 25-4. The individual roller elements were marked with a contrasting paint over one half of the roller end face diameter. This marked end was always on the unnumbered end of the roller. The roller

-37-
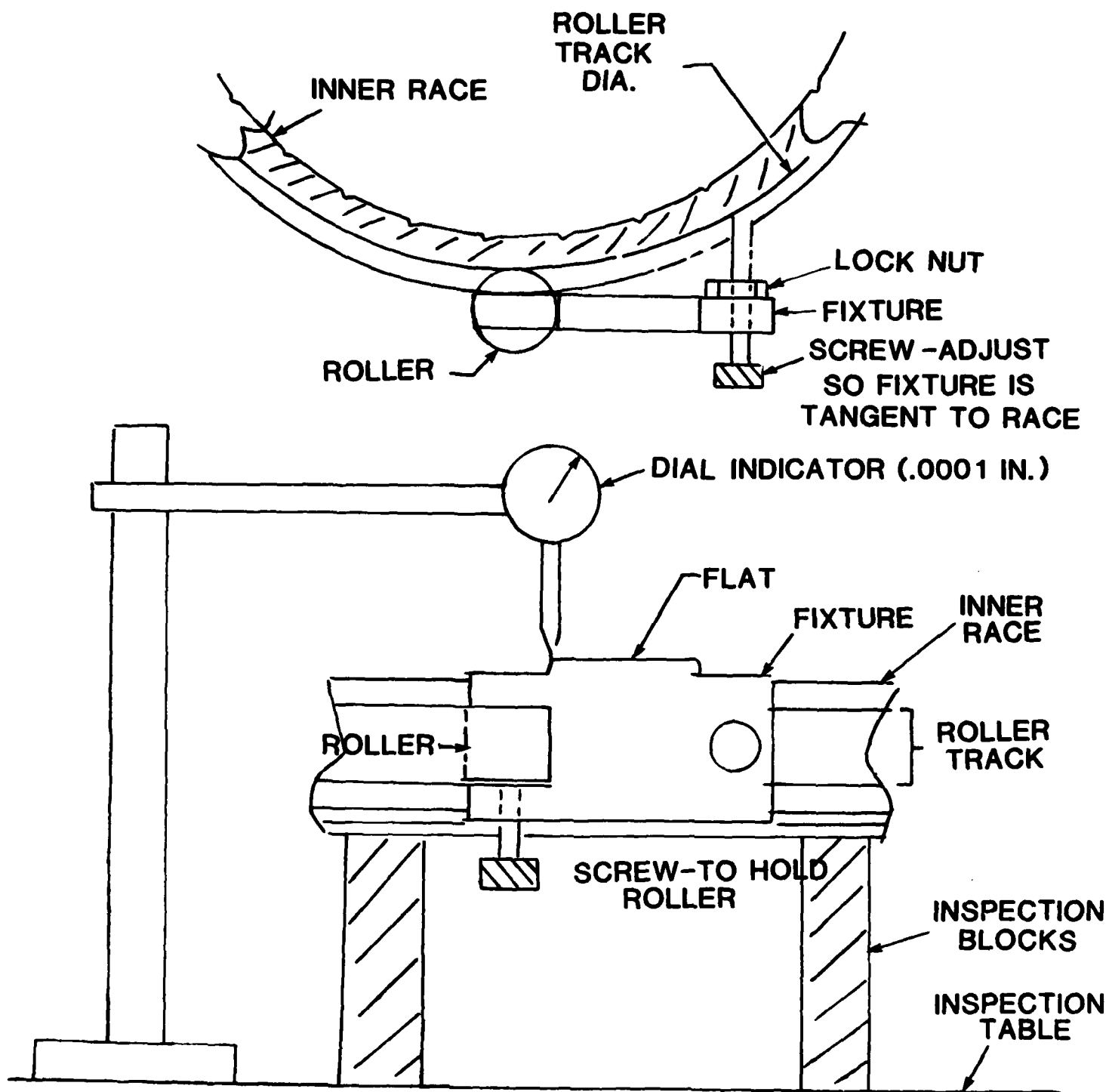
FIGURE 11   SKEW ANGLE FIXTURE

was then spun on its axis and the unbalance associated with each end face plane was measured along with the phase angle relative to the contrasted end face marking. The unbalance measured in mg mm at each plane was then combined using the program referred to in Figure 12.

2.7.2 Epicyclic Motion In a rolling bearing, the elements orbit the bearing axis and at the same time revolve about their own axis. This orbital motion which is coincident with the bearing cage speed was therefore used to establish the epicyclic motion of the bearing. The bearing cage rotational speed was measured by using fibre optics. A two level signal was generated by light reflected off of the side rail of the cage. This bi-level light signal was the result of the difference in reflectivity of the silver and a tarnished (10% sodium sulfide) section of the cage, each consisting of 180 degree sectors of the cage circumference. The change in reflectivity was then converted to an electrical signal recorded on magnetic tape which could subsequently be plotted against a time function to provide a pulsating frequency equivalent to the cage rotational speed.

2.7.3 Roller Spin Speed To determine whether or not rollers in high speed bearings experience pure rolling on the outer race, roller spin speed was measured on several occasions. This measurement was accomplished using two roller spin coils, which are essentially spools of magnet wire and were supplied by "F.A.G". Its operation was dependent upon the magnetically induced alternating

```
    1    PROGRAM
    2    *THIS PROGRAM DETERMINES THE RESULTING VECTOR IN AN UNBALANCED ROLLER
    3    ANGLES IN DEGREES
    4    S1: REQUEST R2
    5    REQUEST THETA2
    6    REQUEST R1
    7    REQUEST R2
    8    Y1=R1*SIN(THETA1)
    9    X1=R1*COS(THETA1)
   10    Y2=R2*SIN(THETA2)
   11    X2=R2*COS(THETA2)
   12    Y=Y1-Y2
   13    X=X1-X2
   14    R=SQRT(X**2+Y**2)
   15    PRINT X
   16    PRINT Y
   17    PRINT R
   18    REQUEST J
   19    IF(J.EQ.1.)GO TO S1
*20    CONTINUE
  :?
```

NOTE: FOR DYNAMIC UNBALANCE MULTIPLY
         R BY ONE HALF THE ROLLER LENGTH

#2
VECTORSCOPE

#1
VECTORSCOPE
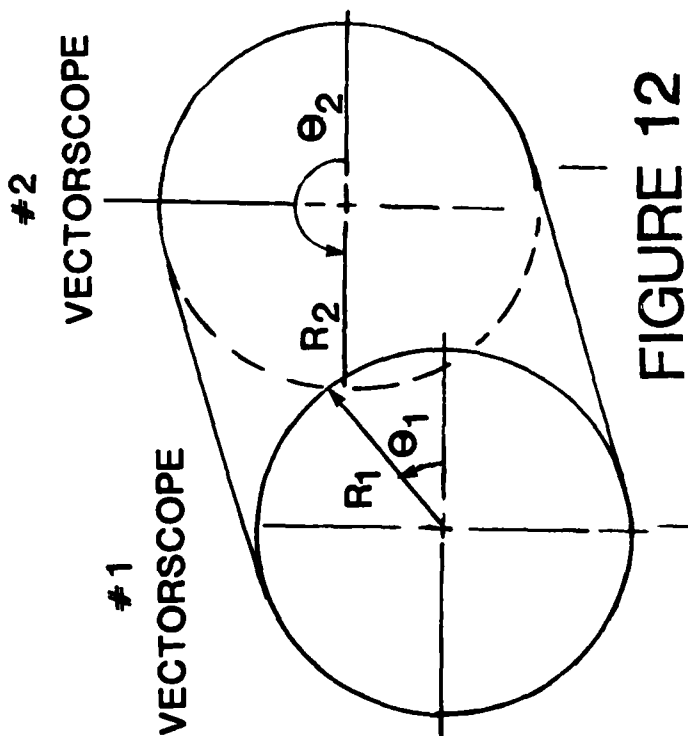
FIGURE 12   ROLLER DYNAMIC UNBALANCE

electrical signal generated by the roller which had previously been magnetized with north and south poles across its diameter. The resulting signal was then amplified and recorded on magnetic tape for subsequent analysis.

2.7.4 Lubrication Effectiveness

2.7.4.1 Oil Scoop Efficiency An investigation of bearing oil flow rates and of the axial oil scoop efficiency was carried out under constant load conditions for the three oil jet flow rates of 5,10 and 15 lb/min. This under-race lubricated bearing was supplied with oil via a rotating annulus formed by a lip on the spanner nut communicating with the bearing through axial slots in the shaft outside diameter.

The test section (FIG 7a) was constructed such that lubricant discharged from the test bearing could be collected separately from that spilled from the axial oil scoop. Comparison of these flows permitted assessment of the efficiency of the lubricant delivery system.

2.7.4.2 Under-Race vs Side Jet Lubrication The test section load bearings were modified to provide under-race lubrication for improved bearing reliability. This modification to the oil supply system provided the means for a comparison of the cooling effectiveness of the systems.

-41-

3.0 TEST RESULTS

3.1 ESK 9244-11

3.1.1 *Roller Weight and Skew Angle Change* The individual roller weights as well as the skew angles were measured and recorded before and after running the 10 hour test. These results are presented in table 6. The individual rollers show an almost negligible weight change with an average loss of .0001 gm. The result of a statistical analysis on roller weight with a 99% confidence level, was that the roller weight change is negligible.

The individual roller skew angle change was more pronounced with an average increase in angle of 2.401 minutes (.000699 radians). Since this skew angle increase is associated with an insignificant roller weight change, it may be that the skew angle increase is guide flange wear rather than roller end wear. Any guide flange wear was not visually detectable. A visual inspection of the roller end faces did not indicate any pronounced wear. What wear was present is of a concentric pattern which would tend to maintain proper roller tracking as opposed to asymmetric wear which has been associated with excessive roller skewing during running and could lead to cage side rail fracture.

-42-

TEST BEARING WEIGHT AND SKEW ANGLE CHANGES
TABLE: 6

BRG NO	ESK 9244-11		ESK 9244-09 (1)		ESK 9244-09A (2)		ESK 9244-03		ESK 9244-10		ESK 9244-09 (3)		ESK 9244-09A (4)		ESK 9244-3 (5)	
ROLL NO	WT GM	SKEW RAD	WT GM	SKEW RAD	WT GM	SKEW RAD	WT GM	SKEW RAD	WT GM	SKEW RAD	WT GM	SKEW RAD	WT GM	SKEW RAD	WT GM	SKEW RAD
1	-.0001	.00025	-.0002	.0095	+.0004	.00264	0.0	-.00052	-.0012	.009	-.0002	.0085	-.0002	.0046	-.029	.0270
2	0	.00113	-.0003	.01015	+.0002	.00264	0.0	.00008	-.0006	.0142	-.0001	.0083	-.0005	.0087	-.0285	.0265
3	0	.000661	-.0002	.0095	+.0001	.00299	-.0001	.00008	-.0004	.0086	-.0001	.0104	0.0	.0083	-.026	.0250
4	-.0001	.000556	-.0007	.01238	0.0	.00254	-.0001	.00034	-.0007	.01619	-.0006	.0123	-.0002	.0037	-.024	.0244
5	0	.000954	-.0002	.00842	+.0001	.00238	-.0001	.00044	-.0009	.0163	-.0002	.0090	-.0002	.0081	-.0203	.0263
6	-.0001	.000547	-.0004	.00974	0.0	.00254	0.0	.00002	-.0003	.0116	-.0002	.0072	-.0001	.0079	-.0186	.0267
7	0	.000652	-.0005	.01197	0.0	.00355	-.0001	.00087	-.0004	.0096	-.0006	.0166	-.0013	.0099	-.0173	.0272
8	0	.000657	-.0002	.00482	-.0012	.00181	0.0	.00007	-.0002	.0110	-.0002	.0163	-.0003	.0042	-.0281	.0277
9	0	.00009	0.0	.01035	-.0008	.00391	-.0001	.00017	-.0005	.0122	-.0002	.0112	-.0008	.0096	-.0179	.0241
10	-.0001	.000602	-.0006	.01172	-.0001	.00218	+.0002	.00054	-.0011	.0130	-.0006	.0131	-.0005	.0047	-.0172	.0282
11	0	.000701	-.0002	.00492	+.0002	.00558	+.0002	.00047	-.0006	.0097	-.0006	.0083	-.0003	.0073	-.0203	.0275
12	0	.000456	-.0002	.00456	+.0002	.00624	-.0001	.00024	0.0	.0132	-.0003	.0084	-.0009	.0043	-.0192	.0268
13	0	.001057	0.0	.01121	+.0002	.00188	-.0001	.00078	-.0002	.0098	0.0	.0099	-.0001	.0046	-.0264	.0250
14	0	.000554	-.003	.00888	0.0	.00279	0.0	.00018	-.0005	.0092	-.0003	.0161	-.0003	.0041	-.0253	.030
15	-.0001	.000957	-.0005	.01243	+.0003	.00431	-.0001	.00059	-.0004	.0139	-.0006	.0130	0.0	.0048	-.0263	.0255
16	-.0001	.000555	-.0002	.01197	+.0002	.00066	-.0002	.00037	-.0003	.011	-.0004	.0121	-.0002	.0035	-.0287	.0255
17	-.0001	.000657	-.0003	.01319	-.0005	.0033	-.0002	.00014	-.0008	.0114	-.0004	.0110	-.0014	.0100	-.0274	.0226
18	0	.000806	-.0003	.00989	-.0002	.0034	+.0001	.00075	-.0005	.0112	-.0002	.0100	-.0025	.0094	-.0203	.0277
19	-.0002	.001208	-.001	.00949	-.0001	.00477	-.0002	.00002	-.0004	.0127	-.0003	.0116	-.0005	.0058	-.0329	.0293
20	-.0001	.001215	-.0003	.00928	+.0001	.00228	-.0001	.00105	-.0003	.0107	-.0002	.3098	-.0004	.0041	-.0476	.0279
21	-.0002	.000609	-.0003	.00857	-.0001	.00315	0.0	.00049	-.0004	.0122	-.0002	.0105	-.0007	.0039	-.0644	.0367
22	-.0001	.000455	-.0003	.01147	+.0001	.00345	0.0	.00065	-.0011	.0154	-.0003	.0109	-.0005	.0036	-.0547	.0265
23	-.0002	.000697	-.0003	.00928	-.0001	.00279	-.0001	.00089	-.0073	.0293	-.0002	.0096	-.0006	.0043	-.0504	.0290
24	+.0001	.00061013	-.0042	.02262	-.0001	.00178	0.0	.00047	-.0104	.0093	-.0054	.0263	-.0006	.0051	-.0446	.0331
MEAN	-.00013	.000699	-.0004	.01042	.0000416	.003065	-.000063	.000144	-.00123	.012429	-.0005	.01170	-.00055	.0061	-.0298	.0281

NOTE:
1. Test Suspended (6 hours)
2. Test Suspended (4 hours)
3. After Test Completion (10 hrs) 28/09/82
4. After Test Completion (10 hrs) 21/10/82
5. After Brg. Failure (7 hrs) 22/12/82

The very small levels of roller weight losses
which occurred after 10 hours of operation coupled with the
very small amount of dynamic unbalance (See Table 7) would
be expected to result in a small skew angle increase as seen
in table 6. This is the case and as seen in the comparison
with other test bearings presented in Table 6, the skew
angle increases are the second lowest exceeding only those
of ESK 9244-03.

3.1.2   Oil Temperature Changes   Figure 13 is a
presentation of the oil temperature changes recorded during
the 5 hour calibration run of 30 points. The plot is the
increase in oil temperature as it had passed through the
test bearing.

Further elaboration concerning the data
generated for this figure must be presented. The first
point is that because of extremely cold test cell ambient
conditions and the length of oil piping supplying the test
bearing, the temperatures at the oil jet nozzle were
significantly below the limits specified in the test
schedule of Table 5. The second point is that the
thermocouples which were located in the oil scavenge lines
were located approximately 3 feet downstream of the test
section. Therefore, some heat loss to the surroundings must
be expected within this length. A final point of
consideration is the heat conduction, within the test
section itself, from the slave bearing section oil scavenge
which collects in this area before being returned to the oil
tank (see figure 7a).

TABLE 7 INITIAL ROLLER DYNAMIC UNBALANCE

| ROLL No	ESK 9244 -11 mgmm²	ESK 9244 -03 mgmm²	ESK 9244 -10 mgmm²	ESK 9244 -09 mgmm²	ESK 9244 -09A mgmm²	ESK 9244 -07 mgmm²
1	1.029000	1.741000	25.509003	124.783997	41.996994	70.778000
2	3.809000	3.053000	25.141993	118.781006	91.195999	78.753998
3	5.090000	2.840000	51.307999	134.727005	135.600006	138.378998
4	2.333000	2.987000	50.792007	49.807999	97.197006	46.785004
5	9.587000	0.463000	31.673996	137.882004	75.556000	47.492004
6	9.149000	12.269000	40.119995	84.778000	94.554993	68.378998
7	8.301000	1.800000	36.845993	101.544006	33.143005	116.395996
8	2.800000	6.543000	49.440994	110.828003	47.147995	140.324005
9	4.212000	0.900000	43.464996	98.272995	18.451004	91.149002
10	3.600000	1.200000	53.358002	42.992004	12.696000	101.171997
11	1.977000	0.600000	56.895004	121.994995	33.283997	79.190002
12	17.070007	2.087000	14.706000	76.867004	38.470993	53.904007
13	2.000000	1.200000	52.334000	85.404999	4.405000	112.794998
14	3.600000	1.587000	55.589996	83.272995	5.199000	37.923004
15	2.948000	2.400000	11.658000	51.966995	29.964005	112.796997
16	1.703000	1.200000	51.167007	64.128006	45.572006	131.927002
17	21.548996	0.900000	30.684998	61.841995	39.378998	135.595993
18	8.981000	1.200000	17.658005	100.677002	48.888000	123.639999
19	2.400000	0.300000	19.798996	60.968002	25.001999	78.268005
20	2.104000	0.300000	27.126999	53.884003	38.242996	57.496994
21	0.467000	0.600000	51.552994	136.753006	42.934006	56.770004
22	5.711000	1.708000	53.949997	101.544998	34.095001	56.697998
23	0.000000	8.619000	61.813004	87.574005	33.867996	56.673004
24	4.236000	8.680000	42.921997	67.537994	26.565994	84.772003
						0.000000
AEV.UNBAL= mgmm²	5.194327	2.715702	39.812927	89.950439	45.558609	86.668991

-45-
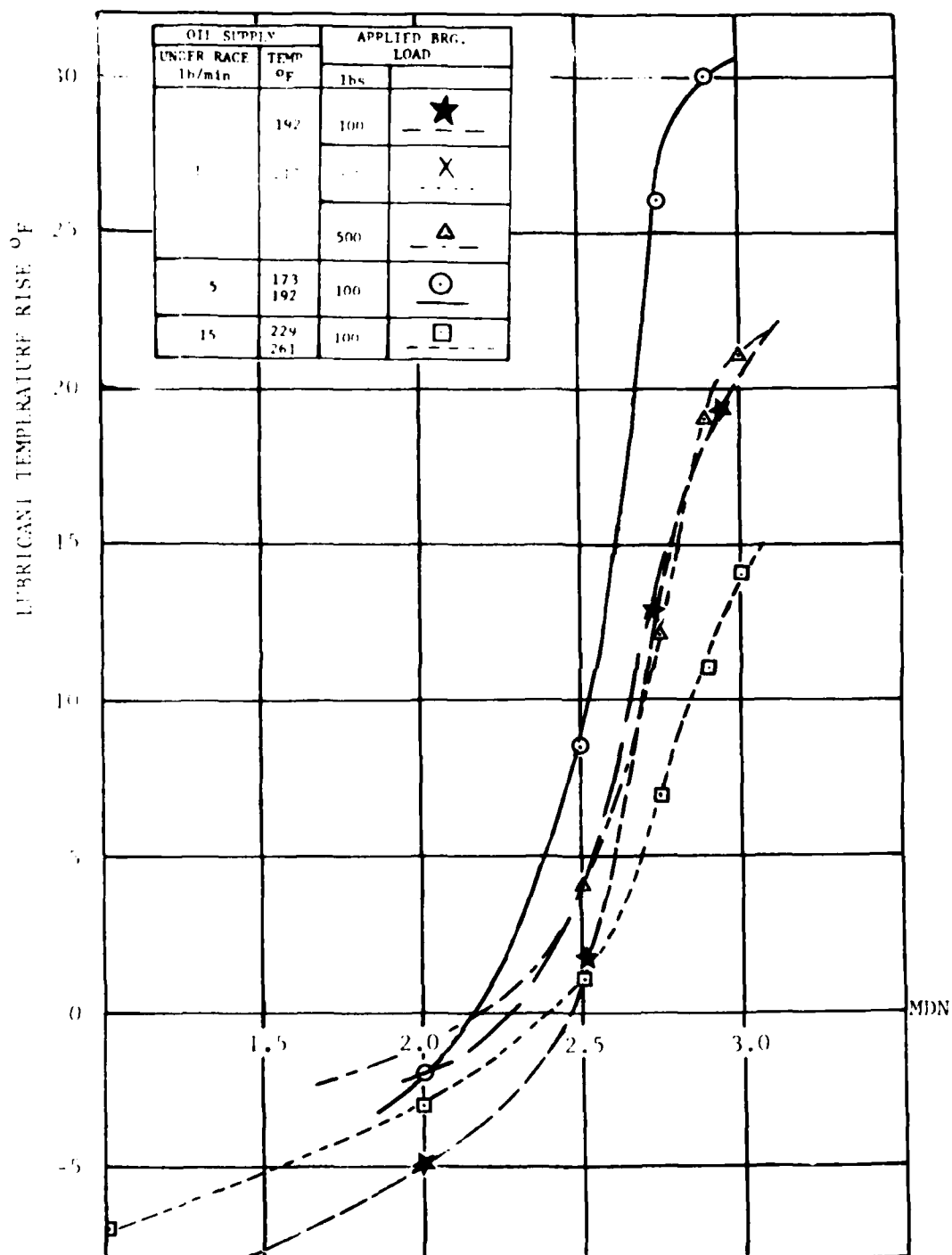
FIGURE 14   OIL TEMPERATURE CHANGE
THROUGH TEST SECTION vs
SHAFT SPEED (ESK 9244-11)

-48-

3.1.3   Bearing Outer Ring Temperature   Test bearing
outer ring temperatures were measured with two thermocouples
(table No.3) with the results presented in figure 15.   The
test results indicate that an oil jet flow rate of 10
lb/min. provides the coolest outer ring temperature
operation at the 3.0 MDN level.   However at speeds below 2.5
MDN, the minimum jet flow rate of 5 lb/min. is most
effective.   The high jet flow of 15 lb/min. is the most
ineffective in maintaining cool outer ring operation.   These
results can be explained by the fact that the high flow
rates of 15 lb/min. would entrain a larger volume of oil
into the bearing than either of the other flow rates.   Since
a major portion of the heat is generated (according to
theory) by viscous drag, it is logical that the high flow
results in the hottest running bearing.   At the other
extreme of 5 lb/min., the oil flow rate is not sufficient to
adequately cool the bearing at the high speed end of the
testing range although it provides for the coolest running
bearing at the low speed range.

Running the bearing with 10 lb/min. jet oil flow
and varying load shows that load is not a significant
parameter for heat generation and has a diminishing
significance at the higher speed range.

3.1.4   Bearing Oil Flow Rates   An investigation of
bearing oil flow rates and axial scoop efficiency was
carried out under constant load conditions for the three oil
jet flow rates of 5, 10 and 15 lb/min.   The results
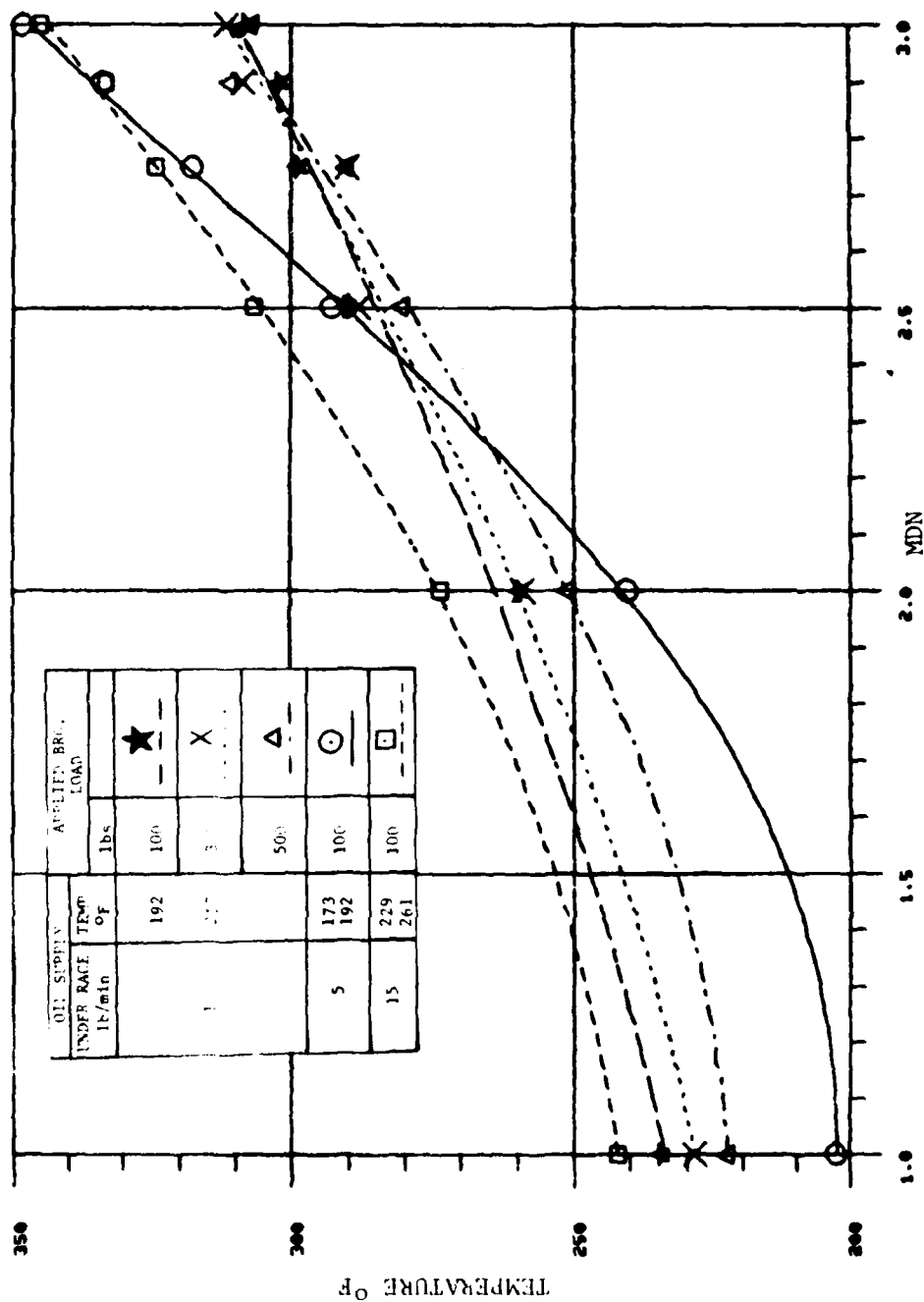presented in figure 16 would indicate that the highest scoop

-49-

FIGURE 15   TEST BEARING OUTER RING TEMPERATURE
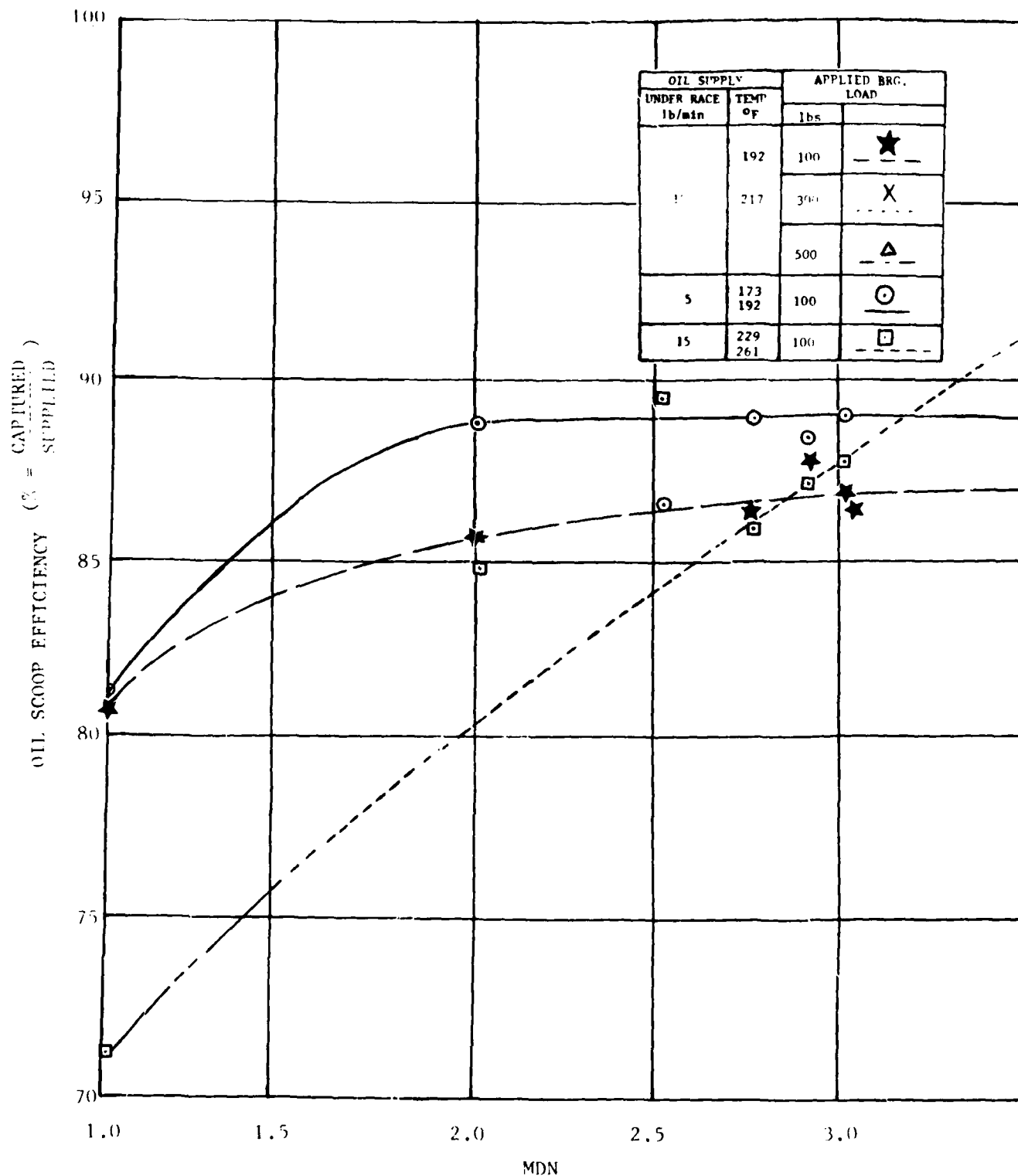vs SHAFT SPEED (ESK 9244 – 11)

FIGURE 16   **AXIAL OIL SCOOP EFFICIENCY vs SHAFT SPEED (ESK 9244-11)**

rejection rate is synonomous with the highest jet flow
rates. In all cases, oil scoop efficiency improves with
increasing speed and is the result of the increased pumping
with the highest overall efficiency gain associated with the
maximum flow rate.

3.1.5 <u>Bearing Cage Speed</u> The results of the bearing
cage speed investigation are presented in figure 17. The
plot considers the effect of varying oil flows and bearing
loads over a range of shaft speeds. The figure is a plot of
percentage cage speed from theoretical epicyclic vs shaft
speed.

Considering only load changes (at a constant
flow rate of 10 lb/min) up to a maximum speed of 3 MDN it
can be seen that the percentage of cage speed for 100 lb,
and 300 lb is virtually identical at 2 MDN and the
difference remains small even at 3 MDN. At the load of 500
lb however and 2 MDN the percentage cage speed (to
theoretical) is about 5% higher, at 3 MDN, all speeds are
virtually identical. The results would imply that a
threshold exists above which slip is dramatically reduced.
As the speed is increased, it would appear that, for the
loads used, the overriding factor is that the cage speeds
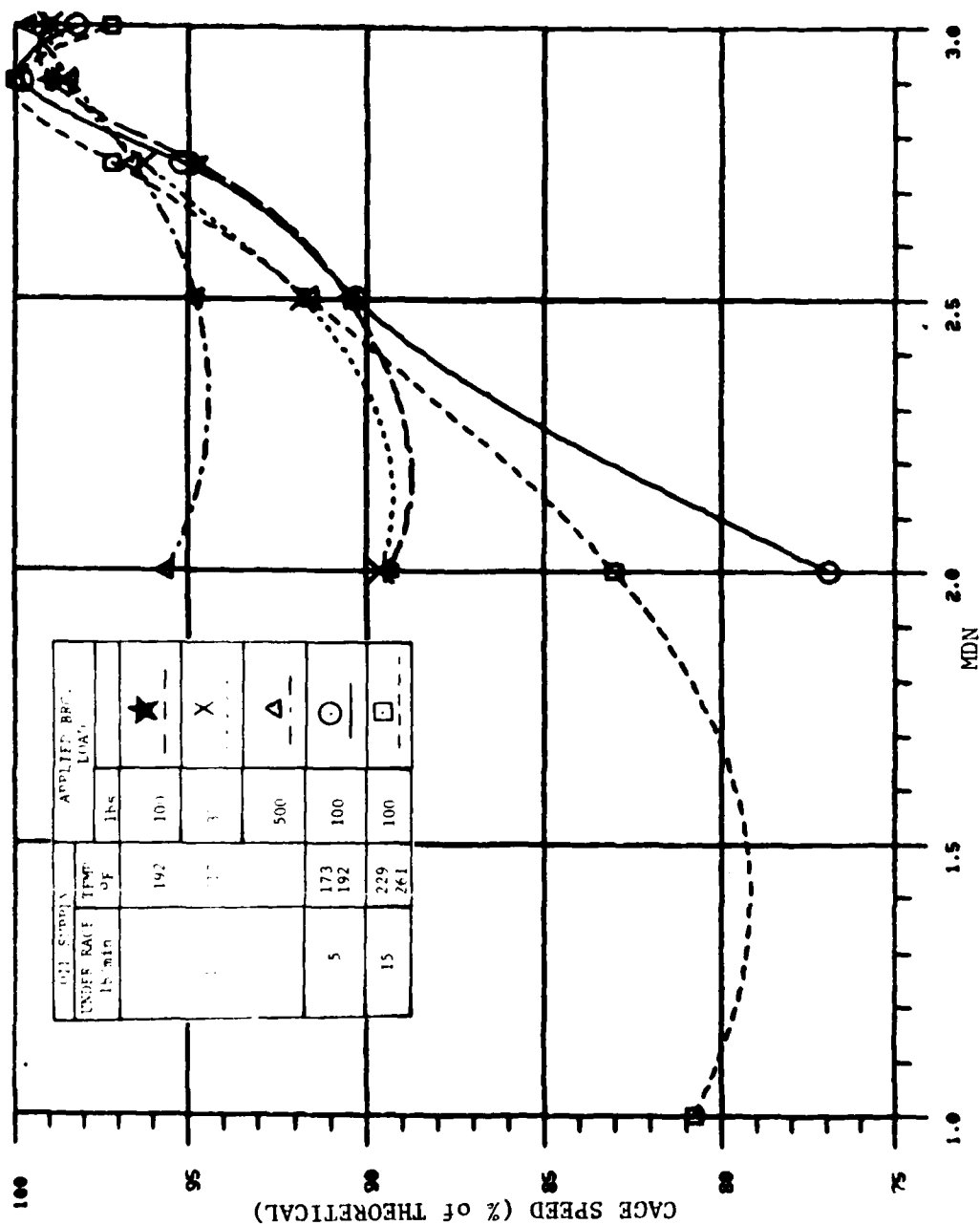are similar irrespective of load or oil flow rates.

-52-

FIGURE 17 BEARING CAGE SPEED vs SHAFT SPEED (ESK 9244-11)

At shaft speeds below 2.5 MDN the cage
speed is shown to also be dependent upon the oil flow
rates. At 2 MDN for instance and 100 lb load, the cage
speed varies from 77%, 89.5% and 83% of true epicyclic for
5, 10 and 15 lb/min. flow rates respectively. As speed
increases however, this difference is reduced and the main
affect seems to be that of speed and is independent of load.

Figure 17 indicates a maximum cage speed
occurring at 2.9 MDN and decreasing at the 3 MDN value. No
viable explanation for this effect has been found.

3.1.6 <u>Bearing Roller Spin Speed</u>   The roller bearing
spin speed data was recorded on tape and the data reduced to
x, y plots maintaining the phase relationship with the
roller frequency and cage frequency. The roller spin speed
data has been reduced and presented in figures 18 and 19.
The figures present the roller spin speeds for different
azimuth positions considering loadings of 100 lb and 500 lb
respectively and cover a variety of speed ranges. It was
expected that the spin speeds would increase as the roller
entered the bearing load zone and then decrease in the
unloaded areas. It is evident that the roller experienced a
wide range of speeds over one entire cage revolution. The
spin therefore does not appear to be a function of roller
azimuth, i.e., load position nor shaft speed cage
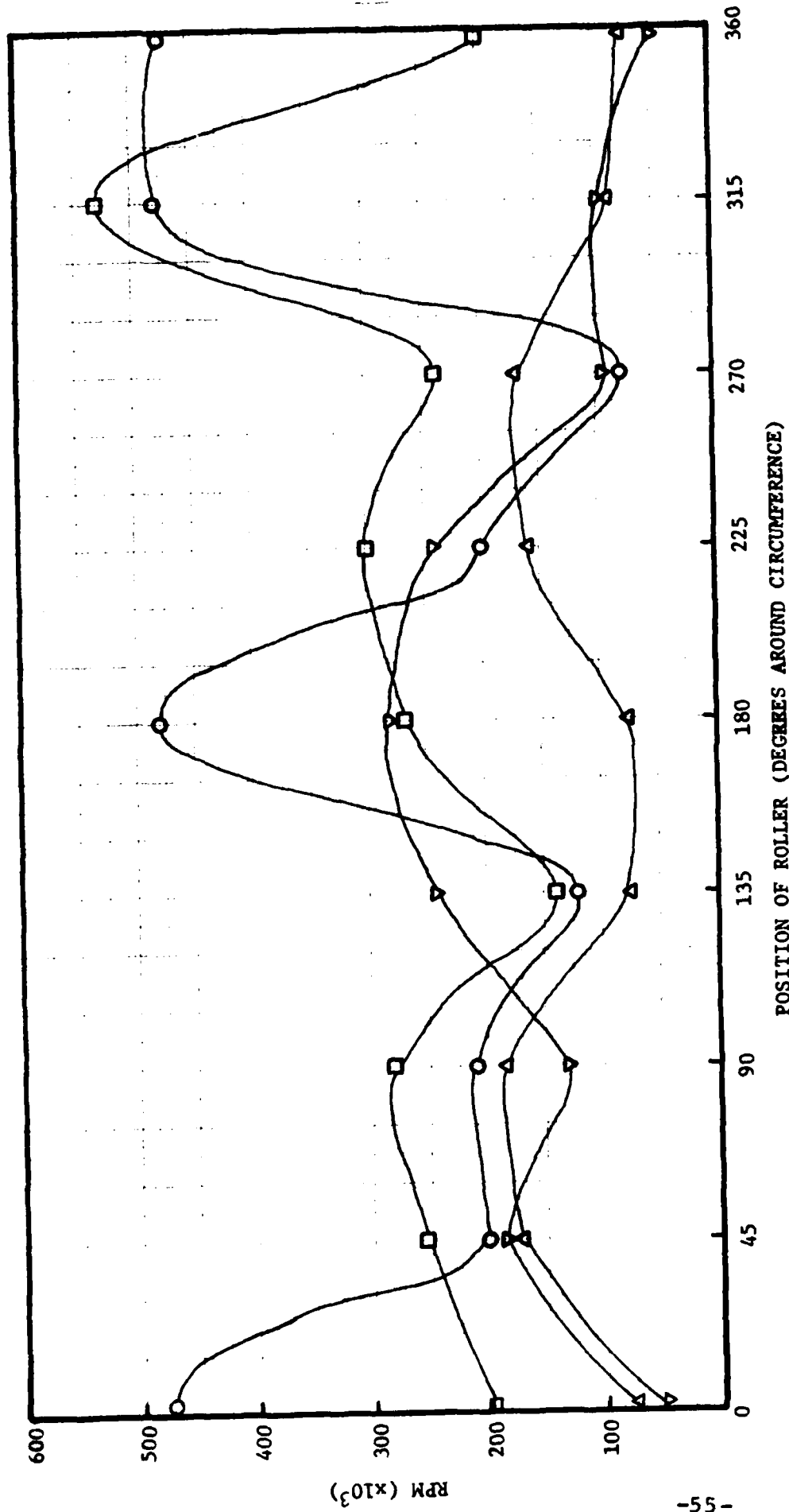revolution.

-54-

FIG. 18
ROLLER SPIN SPEED VS AZIMUTH POSITIONS
(100 LB, RADIAL LOAD)

POSITION OF ROLLER (DEGREES AROUND CIRCUMFERENCE)

RPM (x10³)

△ 2 MDN
○ 2.5 MDN
□ 2.75 MDN
▽ 2.9 MDN

NOTE: ROLLER LOADED AT 180° AZIMUTH

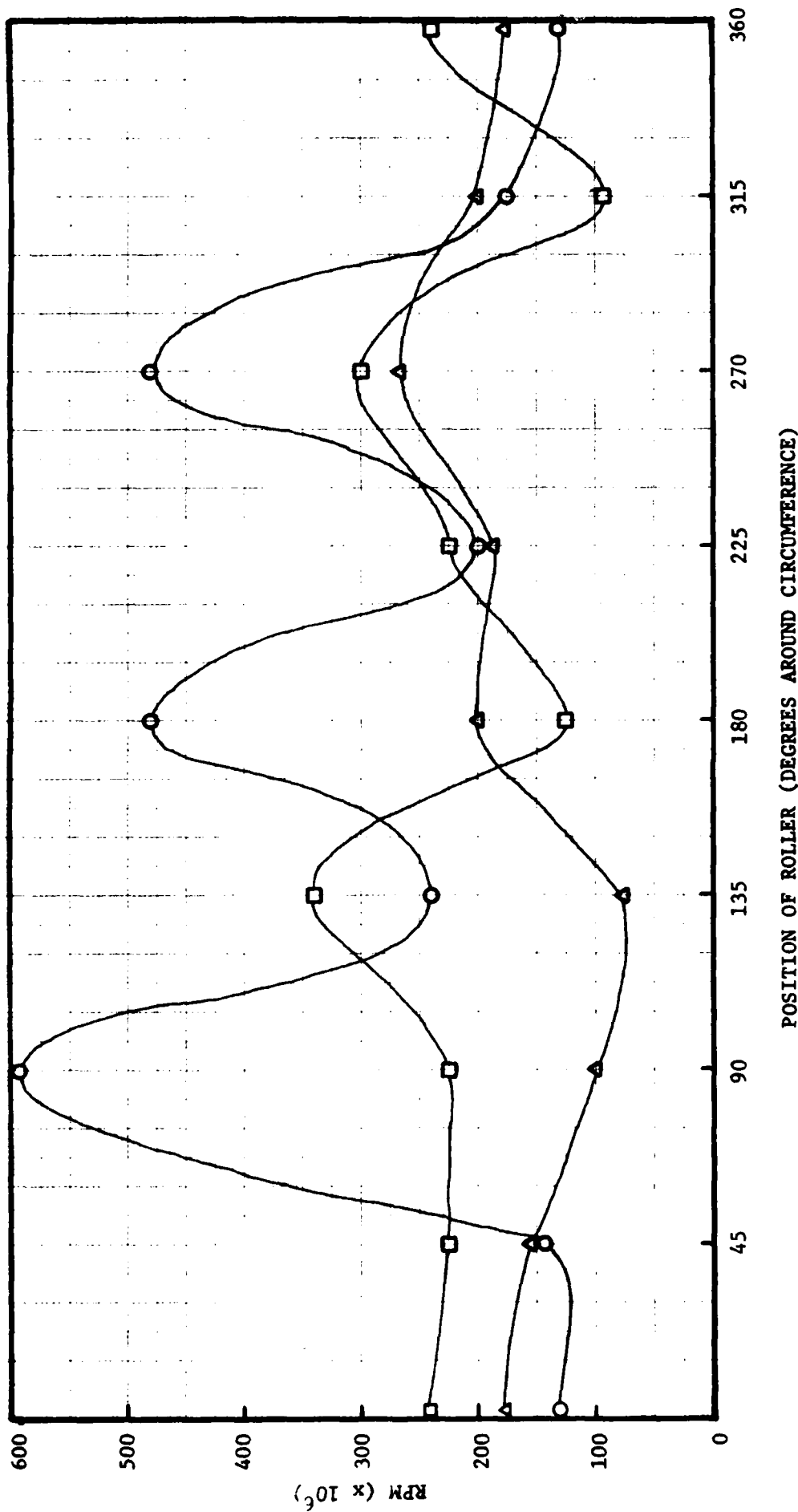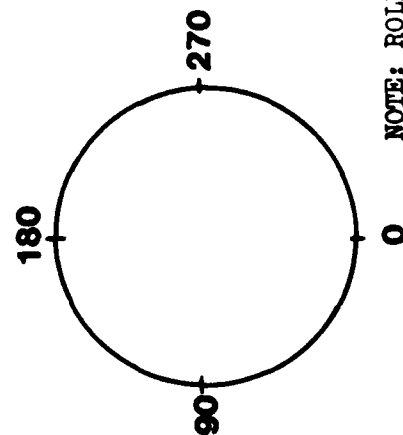POSITION OF ROLLER (DEGREES AROUND CIRCUMFERENCE)

RPM (x 10⁶)
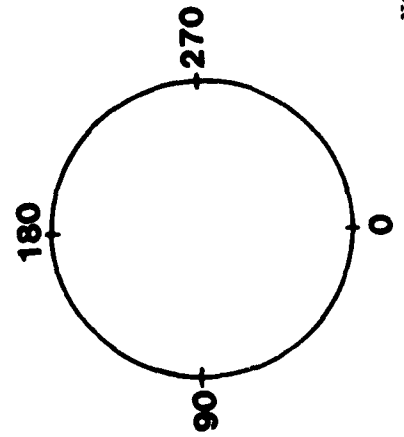
FIG. 19
ROLLER SPIN SPEED VS AZIMUTH POSITIONS
(500 LB. RADIAL LOAD)

△ 2 MDN
○ 2.5 MDN
□ 2.75 MDN

NOTE: ROLLER LOADED AT 180° AZIMUTH

Based on the results of this bearing test, no definitive conclusions can be realized as to the roller spin speed behaviour.

3.2 ESK 9244-03

3.2.1 Roller Weight & Skew Angle Change   The individual roller weights were measured before and after running the 10-hour test and the differences are presented in table 6. The individual rollers show an almost negligible weight change with an average loss of .00006 gm. with standard deviation of .000097 gm.

The skew angles for each roller are recorded both before and after the 10-hour tests. These measurements are carried out with the test bearing inner race and rollers. The roller skew angle change for this bearing is recorded in table 6; an average skew angle change of .495 minute has been recorded.

The total skew angle increase for this bearing is the smallest of all of the bearings tested and is approximately one-fifth of the next smallest skew angle increase. The level of initial roller element dynamic unbalance was also extremely low and is at least one half of the next lowest value. Based on the low levels of initial

-57-

dynamic unbalance (see table 7) and weight change after operation, the low skew angle increase was to be expected.

3.2.2   Oil Temperature Changes   Figure 20 is a presentation of the oil temperature changes recorded using the five (5) hours of "Calibration" running according to the test sequence of table 5.

The oil flow rate of 10 lb/min. with the three radial loadings (see fig. 20) show an increase in temperature with increased loading. In particular, for loadings of 85 lb and 250 lb the variation in oil temperatures is minimal. However, as the loading is increased to 400 lb, a larger temperature increase of 5°F above the previous two lower loading conditions exists which diminishes as the speed approaches 50,000 rpm. Here the predominant factor in oil temperature increase is speed rather than load. In general an oil temperature rise of 50°F occurs over the speed range from 1 MDN to 3 MDN. While temperatures at speeds below 1 MDN remain relatively close to oil inlet temperature.

The minimum oil flow rate of 5 lb/min and a radial loading of 85 lb. results in the largest temperature increase of 64°F at 3 MDN. This is 14°F above the 10 lb/min. flow rate and 16°F above the maximum oil flow of 15 lb/min.
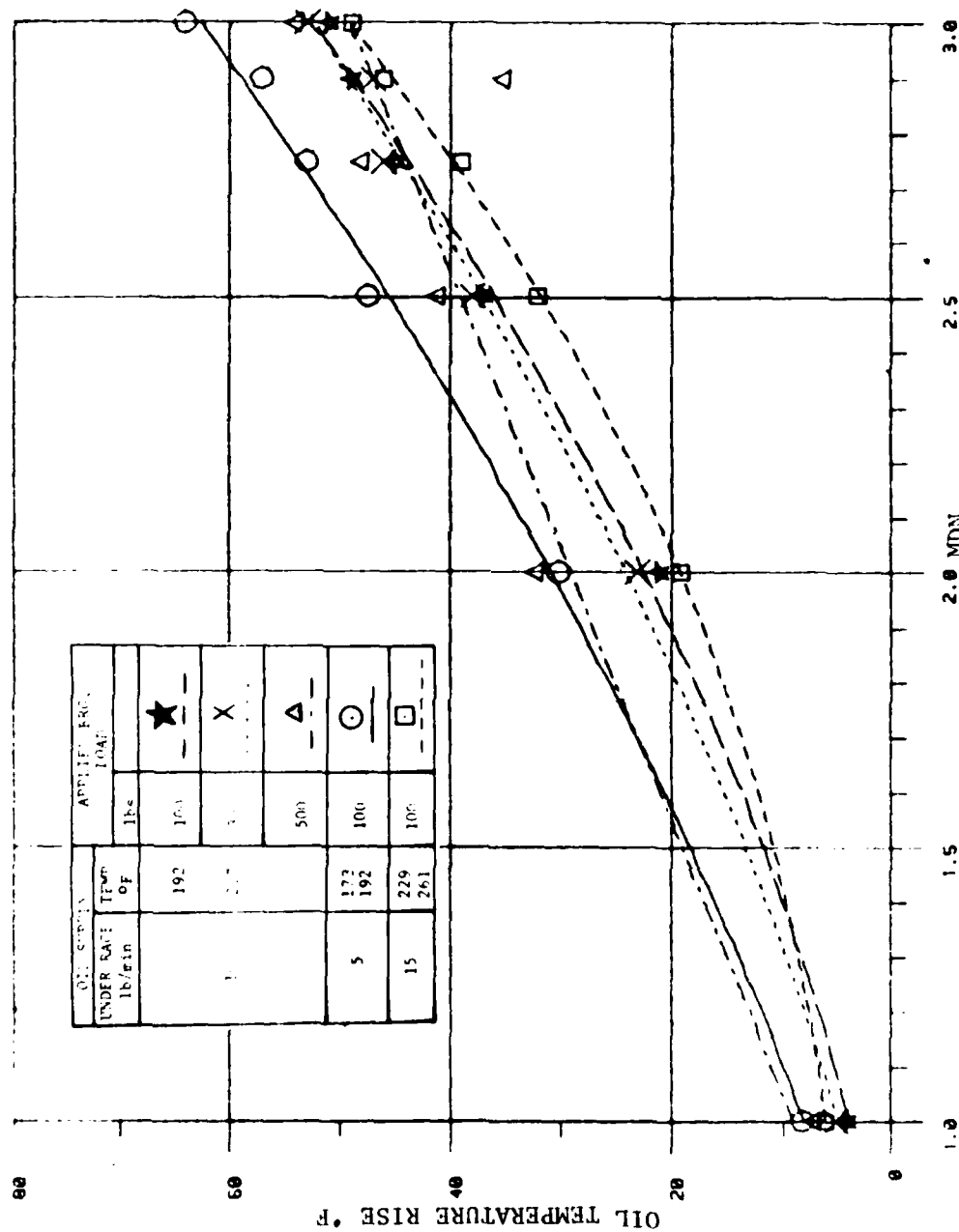
-58-

FIGURE 20   OIL TEMPERATURE INCREASE THROUGH
BEARING vs SHAFT SPEED
(ESK 9244-03)

The temperatures for 10 lb/min. flow and 400 lb radial load is coincident with the 85 lb load and minimum flow (5 lb/min) until 2 MDN. Above this speed, and disregarding the major influence of speed on temperature, loading becomes more influential in increasing oil temperatures, but the predominant factor would appear to be oil flow rates.

The maximum oil flow rate of 15 lb/min results in the lowest oil temperature increase. Although at 3 MDN, the temperature is almost coincident with the 10 lb/min flow, at speed ranges below 1.5 MDN the higher flow rate runs marginally hotter than a 10 lb/min oil flow.

3.2.3   Bearing Outer Ring Temperature   Figure 21 is a plot of the bearing outer ring temperature. The coolest outer ring is associated with the highest oil flow rate of 15 lb/min. for an overall gain of 55°F as compared to 43°F for the oil temperature change of figure 20. The highest outer ring temperature was encountered when the bearing was run with the lowest oil flow of 5 lb/min. In this case the outer ring reached a temperature of 318°F and was rising very sharply at the 3 MDN limit.

In case of a constant 10 lb/min. oil flow rate, the temperatures at 3 MDN increased as the loading increased, although the temperatures for the loadings of 85 lb and 400 lb are only approximately 6°F apart.
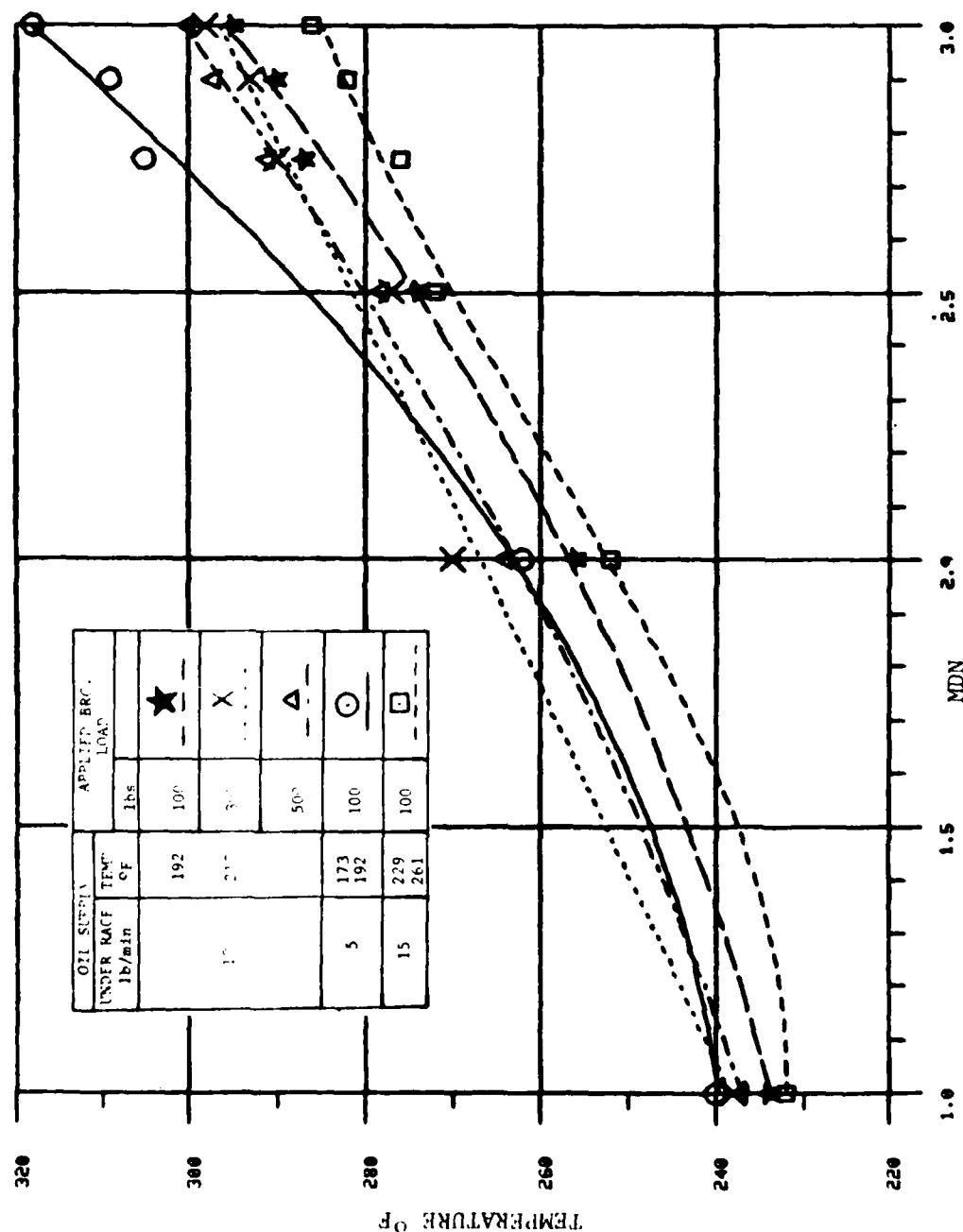
-60-

FIGURE 21 TEST BEARING OUTER RING
TEMPERATURE vs SHAFT SPEED
(ESK 9244-03)

The results of load variation and the constant oil flow of 10 lb/min. would indicate that speed rather than load is the predominant factor for heating of the bearing ring. The variation in flow rates is, however, the major factor with a temperature range, at 3 MDN, of 32°F (from 5 lb/min. to 15 lb/min. oil flow rates).

3.2.4   Bearing Cage Speed   The bearing cage speed is established using a fibre optics probe and a test bearing cage blackened over 180 azimuth degrees. The signal is produced by reflection/absorption and produces a square wave. When the signal is plotted as a time function, the cage rotational frequency is established.

The cage signal strength decreased within the first test points run on the bearing, and was lost within the next several test points. Upon the completion of the bearing test and subsequent rig strip, it was discovered that all cages (i.e, test as well as support bearings) had turned black. It was, therefore, this lack of contrast which prevented the fibre optics probe from functioning.

3.2.5   Roller Spin Speed   Some difficulty has been experienced with this equipment, and shaft speed has been registered rather than the roller spin speed. The source of this anomaly has not been established but it may originate from a residual magnetic field within the rig. The roller spin coils can be connected either in series or in parallel

-62-

and may influence the type of signal frequency received. At
the initiation of the test, the coils were wired and
positioned to generate the strongest signal, and it was not
until data reduction began that the loss of spin frequency
became apparent.

3.3 ESK 9244-10

3.3.1   Roller Weight and Skew Angle Change The
individual roller weight and skew angle changes are
presented in Table 6 and are the results of 10 hours of
operation according to the test schedule. The mean skew
angle increase of .0125 radian is the highest value of the
bearings tested with the exception of ESK 9244-07 which had
terminated in bearing failure. The average weight loss of
the rolling elements of .0012 gm is also the largest loss of
any of the bearings tested, again with the exception of ESK
9244-07. Roller number 12 which did not reflect any weight
loss had a skew angle change approximately one-half of the
calculated mean while still being the second smallest value
of all 24 rolling elements. The largest skew angle increase
was associated with the largest dynamic unbalance (roller
number 23 see Tables 6,7). While the dynamic unbalance of
roller number 12 was approximately one quarter of the mean
value, the skew angle change was only one-half as large (as
the maximum value).

3.4 ESK 9244-09 The testing of the bearing was interrupted after 6 hours of running to facilitate modifications to the test rig assembly. The testing had proceeded to the point of completion of all the calibration running as well as 1 hour of the endurance operation. This opportunity was used to perform geometrically associated measurements of roller weights and skew angles. At the completion of the test schedule, these same bearing parameters were again measured and recorded. It was therefore possible to associate the wear with a particular period of operation (see figure 22).

3.4.1 Roller Weight and Skew Angle Change The results of the skew angle and weight changes are shown in Table 6 after 6 hours of operation as well as at the completion of the 10-hour test. Considering first the results after six hours of operation, the average weight change of .00044 gm includes the effect of three rollers (numbered 9, 11 and 13) which did not show any loss of roller weight. Paradoxically, two of these same rollers had the most significant increase in roller skew angle change. And, at the completion of this test, two of these rollers still did not show a loss in roller weight although roller number 11 almost doubled in skew angle increase. This roller also had the fifth highest dynamic unbalance value. The other roller (i.e roller number 13) which did not change weight during operation showed a slight decrease in skew angle change. This anomaly may have been the result of roller orientation in relation to the wear on the end faces when the measurement was taken. The mean weight lost after 6 hours of operation (60% of the total test time)
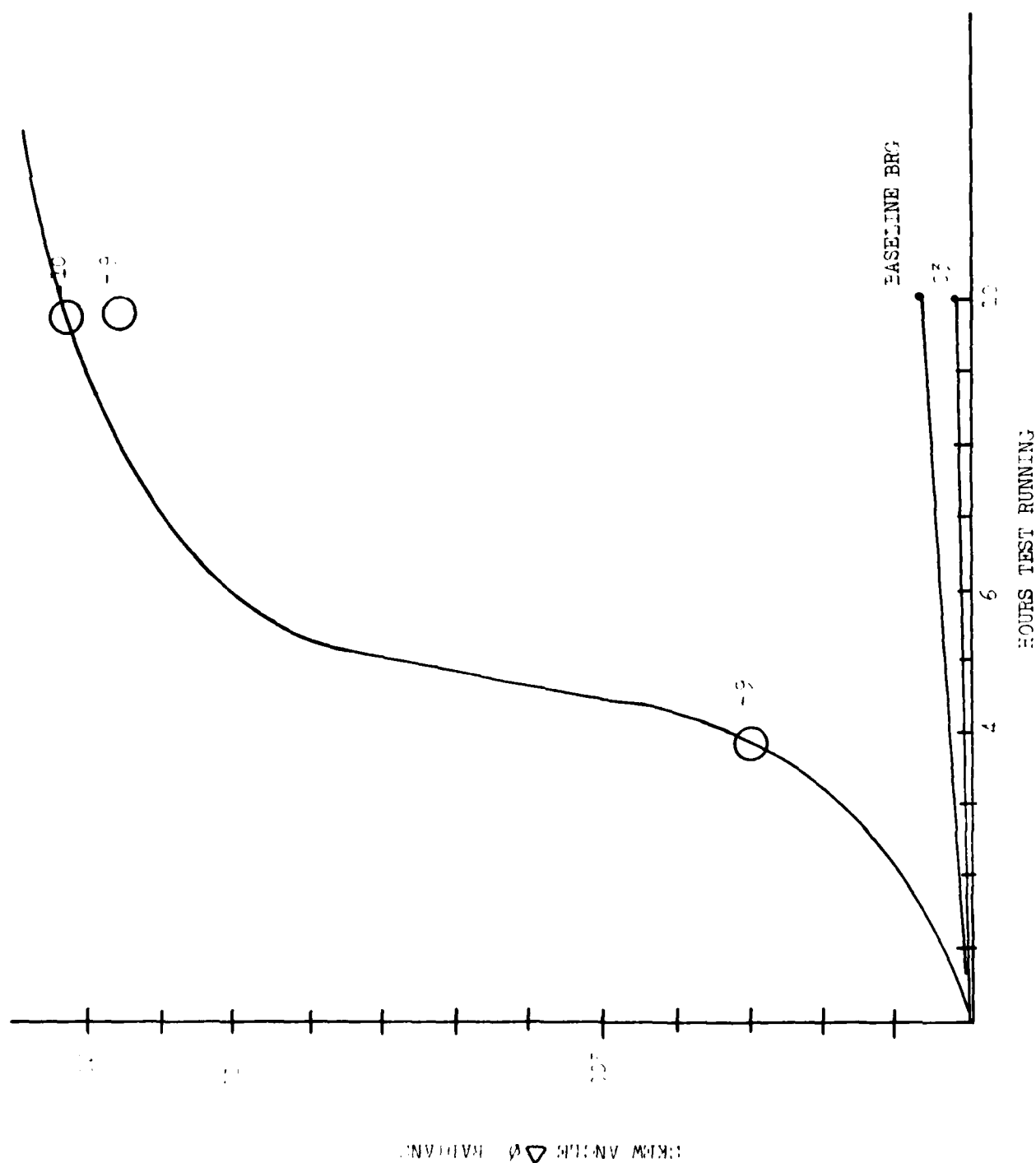
-64-

FIGURE 22
SKEW ANGLE INCREASE vs OPERATING TIME

approached 88% of the total weight loss while the mean skew angle increased by approximately the same percentage of 89%. This would indicate that the roller wear rate is initially very high and is reduced as the testing progresses, suggesting a "wear in" period of operation. The general trend is one of increasing skew angle with increasing unbalance and roller weight loss.

3.4.2 Bearing Cage Speed The results of the bearing cage speed investigation are presented in Figure 23 and consider the effects of variations in radial loads and oil flow rates over the speed range of 1 MDN to 3 MDN.

Considering a constant oil flow rate of 10 lb/min and a variation in loading, the cage rotational speed approaches the theoretical speed confirming the expected result of better roller traction under the influence of the higher load. However, as speeds increase above 1 MDN the cage speed drops off slightly but the higher radial loading still produces cage speeds which are nearer to the theoretical.

At 3 MDN however, the cage speeds corresponding to 400 lb and 85 lb radial load are coincident and marginally above the cage speed associated with the 250 lb radial load. The largest percentage cage slip at 1.0 MDN occurs under a loading of 85 lb with an oil flow rate of 5 lb/min. and is a
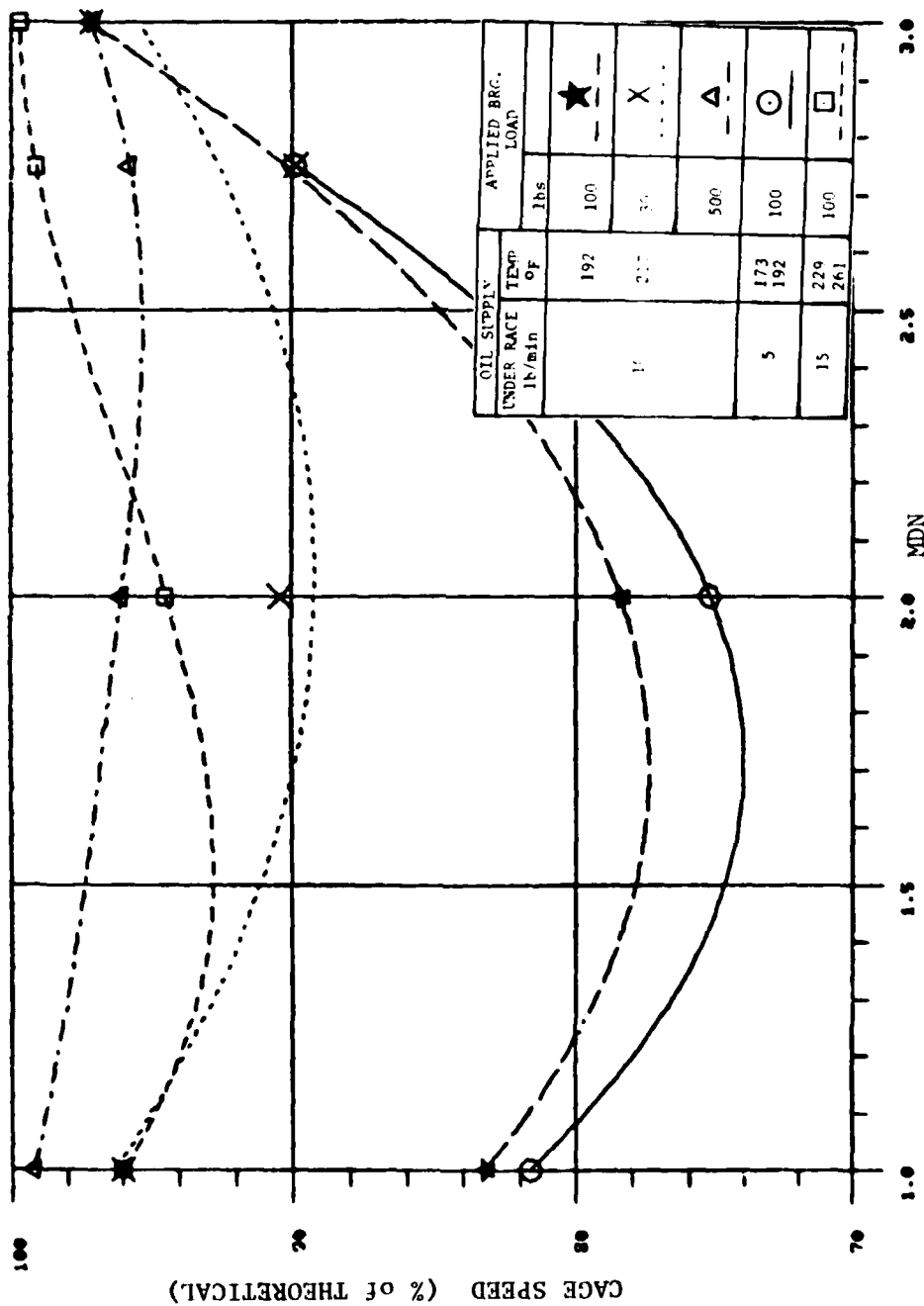
-66-

FIGURE 23   BEARING CAGE SPEED vs
SHAFT SPEED (ESK 9244-09)

few percentage points below the 10 lb/min. oil flow rate
with corresponding loading. The 250 lb load with 10
lb/min. oil supply have coincident points at 1 MDN with the
15 lb/min. oil flow at the lower loading of 85 lb. At 3
MDN, the 15 lb/min. oil flow rate (with 85 lb radial load)
resulted in the highest cage speed. Based on these two
results, it would suggest that either the higher percentage
of oil within the bearing provides additional
circumferential driving force, since the oil is delivered at
inner ring speed, or the extra heat generated within the
bearing as the result of oil churning, has reduced the
bearing internal clearance providing for additional roller
loading. At the extreme speed range of 3 MDN, the
predominant factor influencing cage speed appears to be the
rotor speed since all of the test points are within a few
percentage points of each other.

3.5 ESK 9244-09A The test schedule for this bearing was
temporarily interrupted after 4 hours of operation because
of difficulties experienced in the operation of the test
rig. In this sequence all of the "calibration" running had
not been completed with the operation of 15 lb/min. oil flow
rates outstanding. As in the case of the other interrupted
operation, measurements of weight and skew angle changes
were recorded to provide a graduation of change in these
parameters (see Figure 22).

-68-

3.5.1 <u>Roller Weight and Skew Angle Change</u> The
results of the skew angle and weight changes presented in
Table 6 are measurements taken at the end of 4 hours of
operation and at the completion of the test schedules.
Considering the results after 4 hours of operation, some
instances of individual roller weight increases were
noticed, and have been attributed to errors in measurement
since these values were very small and at the limits of the
instrumentation. The weight change increased by a factor of
10 at the termination of the test while the skew angle
doubled from the measurements taken after 4 hours of
operation. These changes are much more dramatic than those
recorded for test bearing ESK 9244-09 after 6 hours and 10
hours of operation. In comparing these results, it would
appear that operation at 3 MDN, as occurred in ESK 9244-09,
was the major wear period for the bearing.

The results, on weight change, after 10 hours
of operation is virtually identical to that for the similar
bearing ESK 9244-09 tested. In the case of the skew angle,
however, this change appears to be in direct ratio to the
degree of initial dynamic roller unbalance (see table 7) in
each bearing set.

3.6 <u>ESK 9244-07</u> The testing of this bearing was
terminated by the fracture of the cage side rail (see Figure
24A through 24E). The total running time on this bearing
was 7 hours 15 minutes with cage failure occurring after 2
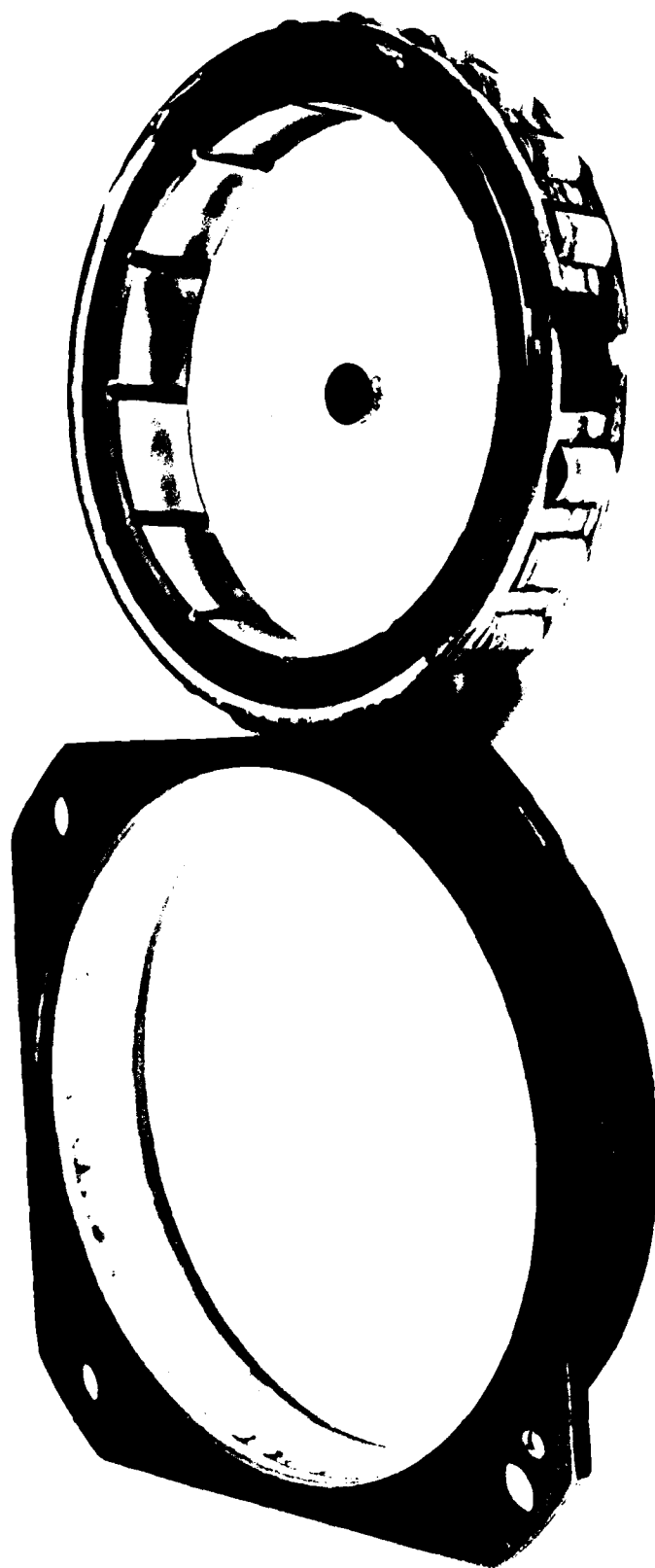
FIGURE 24A   TEST BEARING ESK 9244-07
CAGE FRACTURE (OUTER RING
REMOVED,ROLLER REMOVED)

FIGURE 24B TEST BEARING ESK 9244-07
CAGE FRACTURE (CLOSEUP OF
CAGE FRACTURE)
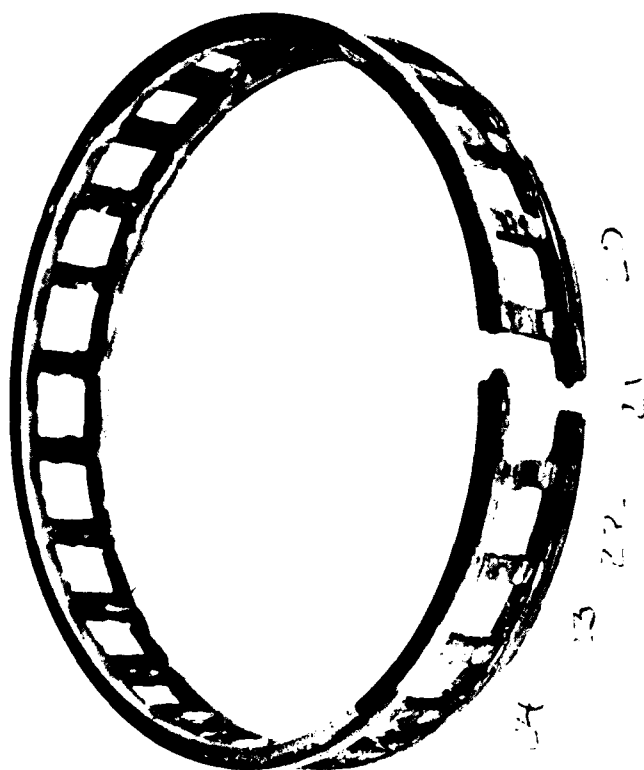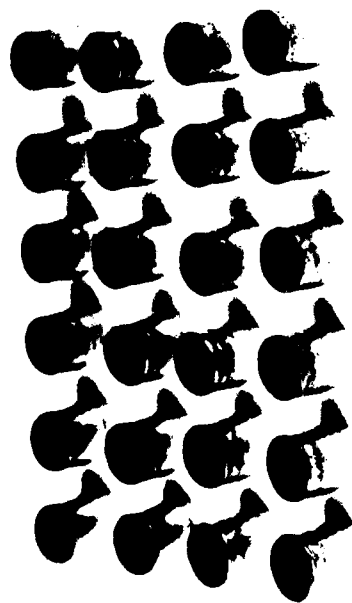
FIGURE 24C   TEST BEARING ESK 9244–07
CAGE FRACTURE(CAGE AND
ROLLER DISASSEMBLED)

FIGURE 24D TEST BEARING ESK 9244-07 ROLLER CAGE FRACTURE (CLOEUP OF ROLLER 21 CYCLINDRICAL SURFACE)
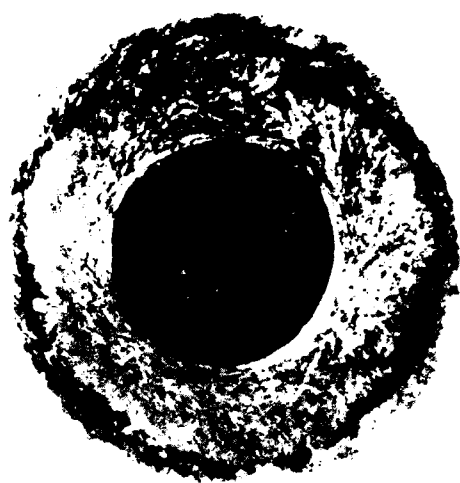
FIGURE 24E   TEST BEARING ESK 9244-07 ROLLER
CAGE FRACTURE (CLOSEUP ROLLER
21 END SURFACE)

and 1 quarter hours of operation in the endurance schedule.
Prior to this, the bearing operation was relatively
uneventful with the only noteworthy occurrences being a 5-
minute run at test point no. 23 before it was terminated due
to high outer ring temperatures, and the elimination of
"calibration" test point no. 24 also due to high outer race
temperatures.

The test rig shutdown was automatic when the
outer raceway temperature reached the pre-set limit values
of 350 °F, maximum temperature recorded were 390 °F and 401
°F (for the two outer race thermocouples located in the
horizontal plane 180°F apart). Simultaneous with the
automatic shutdown, the test operator initiated emergency
shutdown procedures when shaft speed fluctuations were
noticed on the panel readout. The fractured cage was
apparent after the rig was shut down and the front cover
removed. The test bearing was removed for detailed
inspection and recording. The side rails of the cage pocket
containing roller number 21 were fractured and the side
rails on the non-flanged side (of the outer ring) were
approximately one quarter of the original axial width
suggesting wear from contact with the roller end face. Only
the cage pockets on each side of the fractured pocket showed
similar side rail wear and was located on the same side as
well. All of 24 roller elements were heavily pitted over

their entire circumference with roller number 21 (located in the cage pocket with the fractured side rails) showing the most significant diametral change with approximately .005 in. loss in diameter (other rollers averaged .001 loss in diameter). Heavy wear and metal removal were present in the bearing outer race especially toward the flanged side with discoloration indicative of severe over temperature. The inner race showed signs of distress with the pitting over the entire surface being more pronounced on the flanged side of the bearing assembly.

3.6.1 <u>Roller Weight and Skew Angle Change</u> The roller weight and skew angle changes recorded were the result of the 7 hour 15 minute test run and the subsequent bearing cage fracture. Since the final weight and skew angle measurements were made after the bearing failure, it is impossible to assign values of change to normal operation up to the failure point from those associated with the bearing cage fracture. The skew angle increases were remarkably consistent, as is obvious in reviewing the results presented in table 6, with roller number 21 only, being 30% above the average, the weight loss for this roller was much more dramatic at 116% above the average value. The dynamic unbalance of this particular roller however was 35% below the average (see table 7). If it is assumed that the cage side rail wear was the result of roller skewing motion before fracture, then factors other than initial dynamic

unbalance of the roller must be considered. The results
presented in Table 6, because they are measurements taken
subsequent to the bearing failure, must be viewed with
caution, the initial dynamic unbalance however does provide
for valid comparisons. In this case, the average dynamic
unbalance is exceeded only slightly by the highest unbalance
measured which is associated with bearing ESK 9244-09, and
is almost twice as high as the next largest initial mean
dynamic roller unbalance value measured on the duplicate
bearing ESK 9244-09A.

3.7   Bearing Not Tested   Testing on bearing ESK
9244-01 was terminated at point 27 of the calibration
schedule when a failure of the Conrad bearing occurred.
Investigation of this failure revealed a significant design
fault in the test section to drive coupling adapter.
Rectification of this problem would have required extensive
funding beyond contract and it was agreed with the USAF that
the program be terminated at this point and conclusions be
drawn from data already generated.

Bearings not tested as a result of this
decision were as follows:

ESK 9244-01
ESK 9244-02
ESK 9244-08
ESK 9244-06
ESK 9244-09B
ESK 9244-04
ESK 9785-01
ESK 9785-02
ESK 9785-03
ESK 9785-04

3.8   Load Bearing Lubrication   The modification to the
load bearing oil supply system provided the means for a
direct comparison of the cooling effectiveness of the side
jetted and under-race oil schemes.   These results are
presented for the speed ranges of 1.0 MDN to 3.0 MDN.   As is
evident in figure 25, a reduction in the raceway temperature
of approximately 100°F at 3 MDN was achieved by the
employment of under-race lubrication.

4.0   ANALYSIS OF ROLLER END WEAR DATA

In fulfillment of the requirements of reference 1 the
wear data has been subjected to statistical analysis at
P&WA, East Hartford and the results and conclusions drawn
therefrom are detailed in the following report.

4.1   Summary   The present 60 mm bearing data suggests
a qualitative trend in agreement with the 124 mm test
results but does not warrant any modification of the TRIBO 1
wear model.   Any further tests to improve the wear model
should be directed toward:

i)   Clarifying the wear coefficient in relation to
break-in vs steady state and the effects of speed, oil
temperatures, oil flow etc.

ii)   Completion of the test as planned in the original
design experiment, see Table 1 and

iii)   Final correlation of the data resulting from
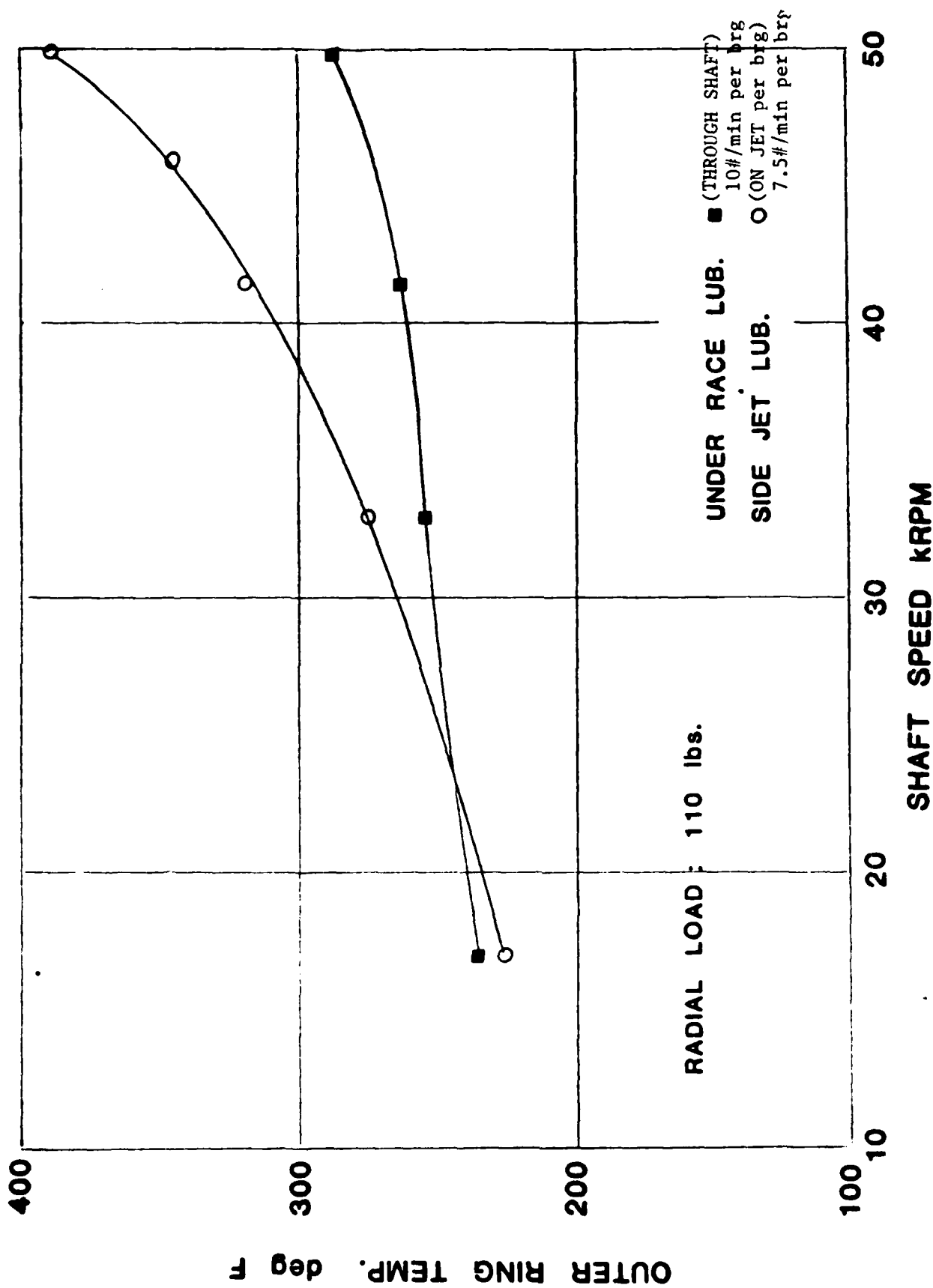these tests with the TRIBO 1 model.

FIGURE 25   LOAD BEARING OUTER RING TEMPERATURE
vs SHAFT SPEED

4.2   Statistical Analysis of Wear Data   The
statistical analysis of the wear results from the small bore
bearing tests was completed.   Table 8 displays the
recommended design experiment test plan for evaluating
the effect of various geometric parameters on the wear
characteristics of 60 mm bearings.   The experiment was
designed to enable separation of the main effects of seven
parameters which would be done by evaluating bearings 1 thru
14, see Table 8.   Furthermore, the effects of two bearing
vendors, FAG and SBB, bearings 6 and 15 respectively, would
be evaluated.   Only six bearings were actually tested,
however with one bearing a repeat, No. 9A, and one bearing
No. 7 having failed.   Table 9 shows the relative level of
the six controlled parameters and corresponding initial
dynamic unbalance.   Inner ring guide flange height was held
at a constant level for these bearings, so it is not
included in the analysis.   Since only four of the 14
recommended bearings were successfully tested, several
parameters were confounded; i.e., concurrent changing of
their relative (high-low) values occurred making it
impossible to deduce one trend as being more significant
than another.   Also in Table 9 are the average wear values
of 24 rollers for the 10-hour test.   The eight parameters
included in the analysis to explore the wear characteristics
are (see Table 10 for actual dimensions):

TABLE 8

RECOMMENDED DESIGN EXPERIMENT

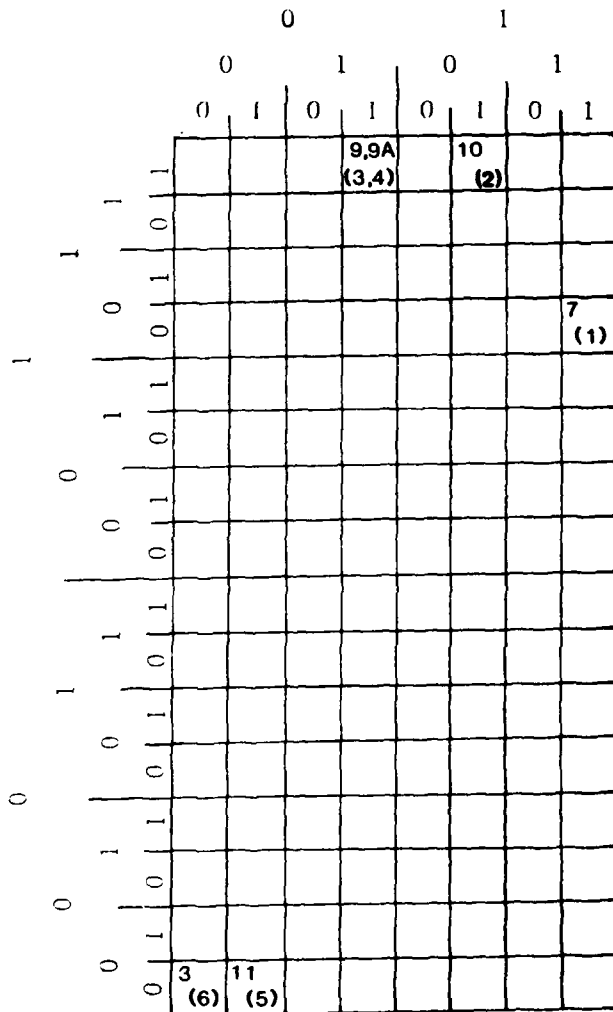|	BEARING			BEARING PARAMETERS				
VENDOR	NUMBER	A	B	C	D	E	F	G
	1	0	0	0	0	0	1	1
	2	0	0	0	0	1	1	1
	3	0	0	0	1	0	0	0
	4	0	0	1	0	0	1	0
	5	0	0	1	1	1	0	1
FAG	6	1	1	0	0	0	0	0
	7	1	1	0	1	1	1	1
	8	1	1	1	0	1	0	1
	9	1	1	1	1	0	1	1
	10	1	1	1	1	1	1	0
	11 (B/L)	0	0	0	1	0	1	0
	12	1	0	1	0	0	1	1
SBB	13	0	1	1	1	0	0	1
	14	1	1	0	0	0	0	0
	15	1	1	0	0	0	0	0

LEGEND

0   —   indicates the low value of the parameter

1   —   indicates the high value of the parameter

A   —   Roller Corner Radius Runout

B   —   Roller End Squareness

C   —   Roller End Clearance

D   —   Inner Ring Guide Flange Height

E   —   Inner Race Taper

F   —   Roller L/D Ratio

G   —   Guide Flange Contour

TABLE 9 — RELATIVE WEAR RANKING (WITHIN MATRIX)

| | | 0 | | | 1 | | | INNER RACE TAPER |
| | | 0 | | 1 | | 0 | | 1 | GUIDE FLANGE CONTOUR |

```
                0        1            0        1         INNER RACE TAPER
            0       1        0       1        GUIDE FLANGE CONTOUR
          0    1   0   1   0   1   0   1      ROLLER L/D RATIO

         ┌───┬───┬───┬───┬───┬───┬───┬───┐
      1  │   │   │9,9A│  │10 │   │   │   │
         │   │   │(3,4)│ │(2)│   │   │   │
         ├───┼───┼───┼───┼───┼───┼───┼───┤
      0  │   │   │   │   │   │   │   │ 7 │
         │   │   │   │   │   │   │   │(1)│
         ├───┼───┼───┼───┼───┼───┼───┼───┤
         ...
      0  │ 3 │11 │   │   │   │   │   │   │
         │(6)│(5)│   │   │   │   │   │   │
         └───┴───┴───┴───┴───┴───┴───┴───┘
```

KEY: Block includes bearing
number and, in par-
enthesis, the relative
wear ranking

9A is a repeat of 9.

0 – low runout value

1 – high runout value

ROLLER CORNER RAD. R/C
ROLLER END CLEARANCE
ROLLER END SQUARENESS
INITIAL DYN. UNBALANCE

Bearing	Average Weight Loss (grams)	Average ΔSkew (radian)	Relative Wear Rank
3	.00006	.0002	(6)
7	.02982	.0281	(1)
9	.00050	.0117	(3)
9A	.00060	.0061	(4)
10	.00123	.0124	(2)
11	.00011	.0007	(5)

TABLE 10

ACTUAL BEARING DIMENSIONS

BEARING PARAMETER	3	7	9	9A	10	11
Roller Corner Rad. R/O	.0018	.0692	.0692	.065B	.0708	.0016
Roller End Squareness	.0005	.0081	.0084	.0048	.0104	.0005
Roller End Clearance	.024	.028	.078	.070	.069	.027
Inner Ring G.F. Ht.	70.072	70.096	70.095	70.086	70.087	69.737
Inner Race Taper	.172	3.438	.630	.458	3.323	.573
Roller Length	6.004	8.003	8.008	8.004	8.008	8.004
Guide Flange Contour	Flat	Round	Round	Round	Flat	Flat
Initial Dyn. Unbalance	2.716	86.669	89.950	45.560	39.810	5.194

All parameters are measured in "mm" except Inner Race Taper (minutes) and Initial Dynamic Unbalance ($mg\text{-}mm^2$)

A. Roller Corner Radius Runout

B. Roller End Squareness

C. Roller End Clearance

D. Inner Ring Guide Flange Height

E. Inner Race Taper

F. Roller L/D

G. Inner Ring Guide Flange Contour

H. Initial Dynamic Unbalance

Key observations from Table 9 are: (a) the data available for analysis is sparse resulting in confounded effects, (b) parameters A, B, and H increase concurrently as relative wear increases, and (c) parameter E increases as relative wear increases.

The main parameters affecting high speed roller bearing life are considered to be average roller weight loss and average skew angle change and will therefore be used to evaluate and rank the roller bearing variables tested. For the statistical analysis these two dependent variables are expressed as follows:

Y_1, Average Weight Loss

Y_2, Average Skew Angle Change

Multiple regression equations were developed from the experimental weight loss and skew angle change data by the method of least squares. Each equation yields the mean value of one of the dependent variables. The equations,

therefore, yield the expected wear performance of a roller bearing under specific operating conditions. Prior to the development of the actual regression equations, a mathematical model was in each instance formulated relating the independent variables to the dependent variable. The general form of the model is a multivariate polynomial in which the coefficients appear linearly. The terms in each model are candidates for inclusion in the fitted regression equation.

The general model takes the form:

$$Y = B_0 X_0 + B_1 X_1 \ldots + B_n X_n + e = \hat{Y} + e$$

where Y is the observed value of a particular dependent variable, either Y_1 or Y_2, $\hat{Y}$ is the observed value of the dependent variable computed from the expression involving the X and B terms, where the X terms are the value of the independent variables, the B terms are the coefficients to be estimated from the experimental wear data, and e represents the difference between the observed and the estimated value of the dependent variable due to the residual variation or experimental error in the observations.
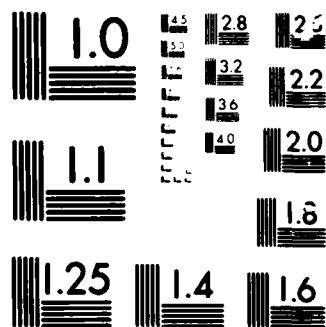
MICROCOP CHART

The regression analysis was performed both with and without bearing 7 since it is not known how the failure affected the magnitude of the wear characteristics. These data sets were analyzed in order to determine the values of the regression coefficients as well as other statistics. The regression models developed for each dependent variable, Y_1, and Y_2 are shown in the tabulations below. The information presented includes;

. Variable name

. COEFFICIENTS: Calculated values of the regression coefficients

. SIGNIFICANCE LEVEL: The numerical percentage describing the significance of a cause (independent variable) and effect (dependent variable) relationship. The higher the percent, the more statistically meaningful the relationship.

. PERCENT VARIABILITY EXPLAINED: R^2, which is the square of the multiple correlation coefficient R, is a measure of the proportion of variation in the dependent variable accounted for by the regression equation. The closer R^2 is to 100% the greater the accuracy of the prediction equation.

. SEE, or Standard Error Estimate, is the magnitude of
  the error for the prediction of the dependent
  parameter. Regression analysis minimizes the SEE
  value where

$\hat{Y}$ is the calculated value of the dependent variable
based on the regression equation

Y is the actual value of the dependent variable

and

$$\hat{Y} - SEE \leq Y \leq \hat{Y} + SEE \qquad 68\% \text{ of the time}$$

$$\hat{Y} - 2 \, SEE \leq Y \leq \hat{Y} + 2 \, SEE \qquad 95\% \text{ of the time}$$

$$\hat{Y} - 3 \, SEE \leq Y \leq \hat{Y} + 3 \, SEE \qquad 99.7\% \text{ of the time}$$

where the actual value will be contained within the
interval of Y + K SEE a given percent of the time.

. R, the correlation between Y and $\hat{Y}$, is an index
  indicating the degree of association between $\hat{Y}$ and Y,
  where a value of 1.0 indicates a perfect fit, i.e.,
  no experimental error, and a value of 0 indicates no
  association, i.e., large experimental error.

. N is the sample size

4.2.1 Multivariate Linear Regression Without Bearing 7

Dependent Variable	Independent Variable	Intercept	Coefficient and Significance Level		% Variability Explained	See	R	N	Figure
Average Weight Loss	Roller Corner Radius Runout	0.00006	0.0105	(91%)	67.4	0.00031	0.821	5	29
	Roller End Clearance	-0.00022	0.0104	(85%)	55.0	0.00036	0.742	5	30
	Roller End Squareness	0.00084	0.0939	(96%)	81.1	0.00024	0.901	5	26
	Initial Dynamic Unbalance	-0.00028	0.000006	(75%)	20.4	0.00048	0.452	5	31
Average Skew Angle Change	Roller Corner Radius Runout	-0.00011	0.1495	(98%)	86.1	0.0026	0.928	5	32
	Roller End Clearance	-0.00510	0.2098	(97%)	84.6	0.0027	0.920	5	33
	Roller End Squareness	-0.00026	1.3008	(99.9%)	98.4	0.0009	0.992	5	27
	Initial Dynamic Unbalance	0.00107	0.00014	(92%)	69.5	0.0038	0.834	5	34

The above regression equations demonstrate that Roller End
Squareness is only slightly more significant than the other
three parameters with which it is confounded. This
comparison will not be done for the following equations
since two independent variables have been included, making a
similar comparison very difficult.

4.2.2 Multivariate Linear Regression Including Bearing 7

- For Average Weight Loss - No significant regression
  possible because average weight loss for bearing 7 is
  20 times that of the next largest.

- For Average Skew Angle Change (Figure 28)

	COEFFICIENT	SIGNIFICANCE LEVEL
Constant	-0.00286	
Inner Pace Taper	-0.00385	95%
Initial Dynamic Unbalance	0.00016	95%
Percent Variability Explained	= 93.0	SEE = 0.00357 radians
R = 0.964	N = 6	

The significance level permits the evaluation of each
term in the response regression equation with a value $<$ 80%
indicating no significant effect and a value $\geq$ 99%
indicating a very strong bearing variable. Those
independent parameters not included in the regression models
were either not statistically significant, or correlates

with a parameter already in the equation (confounded).

Figures 26, 27 and 29 thru 34 show graphic representations of the single-variable equations. Figure 28 exhibits the best fit line through the data for initial dynamic unbalance at both high and low levels of inner race taper.

4.3   TRIBO 1 and the Wear Model

TRIBO 1 is a state-of-the-art cyclindrical roller bearing design tool developed by P&W under contract with the Navy and Air Force in the High Speed Roller Bearing Program, References 1 and 2.   The program is composed of two basic modules - STATIC and SYSDYN.   The module SYSDYN is, in turn, composed of the modules CADYN and RODYN.   Figure 35 shows the relationship of the modules to each other and to the complete program.

STATIC is the module containing the structural analysis of the bearing due to loads resulting from quasi-static equilibrium.   RODYN is the module that analyzes roller dynamic behavior without the influence of the element retainer or cage.   CADYN is the module that analyzes the cage dynamic behavior without the influence of the rollers. The module SYSDYN analyzes the complete system dynamic behavior allowing full interaction among the rollers, the cage, and the two raceways.   The complete program, TRIBO 1, is employed by running the modules STATIC and SYSDYN together so that the output from STATIC is used as input to the module

-90-

SYSDYN.STATIC may also be run to provide input for the module RODYN.

The computer program was constructed in a modular fashion to maximize flexibility and efficiency and to allow for partial analysis, wherein a certain aspect of the analysis may be considered separately in order to save computation time.

TRIBO 1 requires input information which specifies significant geometry features of the bearing such as corner radius, guide flange layback angle and end clearance. Each of these geometry variables has an effect on the overall force system acting on the rollers and cage and thus affects the dynamic motion of the bearing. As bearing diameter increases or decreases from some reference value, the relative importance of one geometry feature compared to any of the others may change. For example, parameters such as roller diameter and length which affect the overall mass of the roller may increase considerably if the bearing radius is doubled, while roller end clearance which affects the dynamic damping at the roller ends remains relatively constant.

TRIBO 1 has been correlated for 124 mm roller bearings under contracts N00140-76-C-0383 and N00140-81-C-4800. The wear data generated from the parametric testing conducted under these contracts has been incorporated into the TRIBO 1 wear model as described in reference 1. Updates to the model, reference 3, included the effects of corner radius runout and end runout on both dynamic behavior and wear.

In each of the previous contracts, the relative
importance of each parameter with regard to the overall
dynamic behavior of the bearing, including its wear rate, was
well established via testing. Since the dynamic motion of
the bearing as modeled by TRIBO 1 was also correlated to the
same test data, there is a high degree of confidence that the
output roller motion and wear prediction are realistic for
bearings of similar size run at similar speeds.

Because of the small number of bearings successfully run
for the 60 mm program, it is not possible to statistically
separate the effect of each geometry parameter on the overall
motion or resulting wear. Thus, a comparison cannot be made
with the previous 124 mm data to determine if any changes in
the relative ranking of the individual geometry variables has
occurred. Without such a comparison, modification of the
existing TRIBO 1 wear model would not be meaningful and is
not recommended.

Review of the limited amount of data available does not
indicate that any significant changes in the relative
importance of any of the tested parameters has occurred with
the reduction in bearing diameter to 60 mm. Thus, basic
trends identified in the original TRIBO 1 wear correlation
based on 124 mm bearing data have been confirmed by the 60 mm
test data but further quantification of the wear coefficients
in the analysis to reflect small bearing operation is not
practical under the current circumstances.

The present TRIBO 1 wear model is based on the applicability of Archard's Law of wear on impact sliding during roller and guide flange metal to metal contact. Archard's Law of Wear states that the wear

$$W_i = \frac{K \, P_i S_i}{3H} \tag{1}$$

is produced whenever a contact occurs in the dynamic system. The total wear is then the sum

$$W_{total} = \sum_i \frac{K \, P_i S_i}{3H} \tag{2}$$

where

W = wear volume (inch^3)

P = load (lb) = impact force

S = sliding distance (inch)

H = Brinell hardness

K = empirically determined wear coefficient

While H is a material constant and P and S are calculated from the SYSDYN module of TRIBO 1, K is determined from test data and depends on whether the contact occurs during the break-in period or during steady state operation.

The parametric study of the 124 mm A/F bearings revealed
that the roller coupled corner radius run out is the most
significant parameter followed by the roller end clearance
and roller squareness. Of course the end effect of the
corner radius runout and the end squareness is the roller
unbalance which produces the skew force. Thus, roller
unbalance and end clearance have the most significant effect
on normal roller wear. This qualitative trend is not
difficult to understand. Its quantitative aspect requires
test data for model correlation purposes.

In the present 60 mm roller bearing study it was also
found that the most significant effect on roller wear comes
from the corner radius runout, end squareness, initial
unbalance and end clearance. Again, the roller unbalance and
the roller end clearance provide the most impetus to the
normal roller wear - the same qualitative trend established
in the 124 mm bearing program.

Test data from the 60 mm bearings is, however, rather
limited. It consists of two distinct sets for 10 hr wear
data - one with high roller unbalance and large end clearance
and the other with low roller unbalance and small end
clearance. Since intermediate wear data is not available,
the characteristic wear coefficient relating to the break-in
period as distinct from steady state operation is not known.
Even if one assumes the same wear coefficient for both
operating modes, the fact that the effects of roller
unbalance and end clearance are confounded does not provide
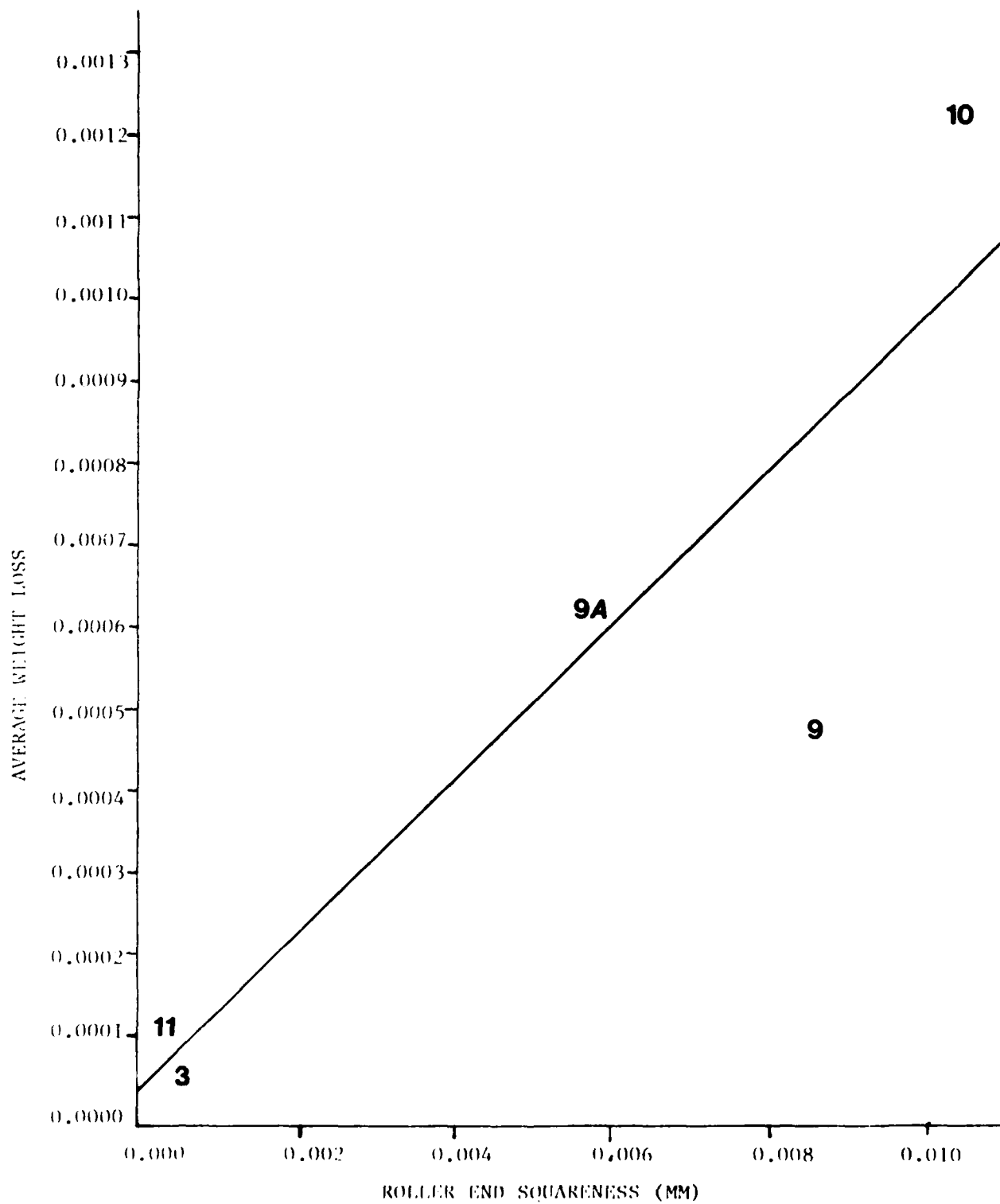the information necessary to identify the independent
effects.

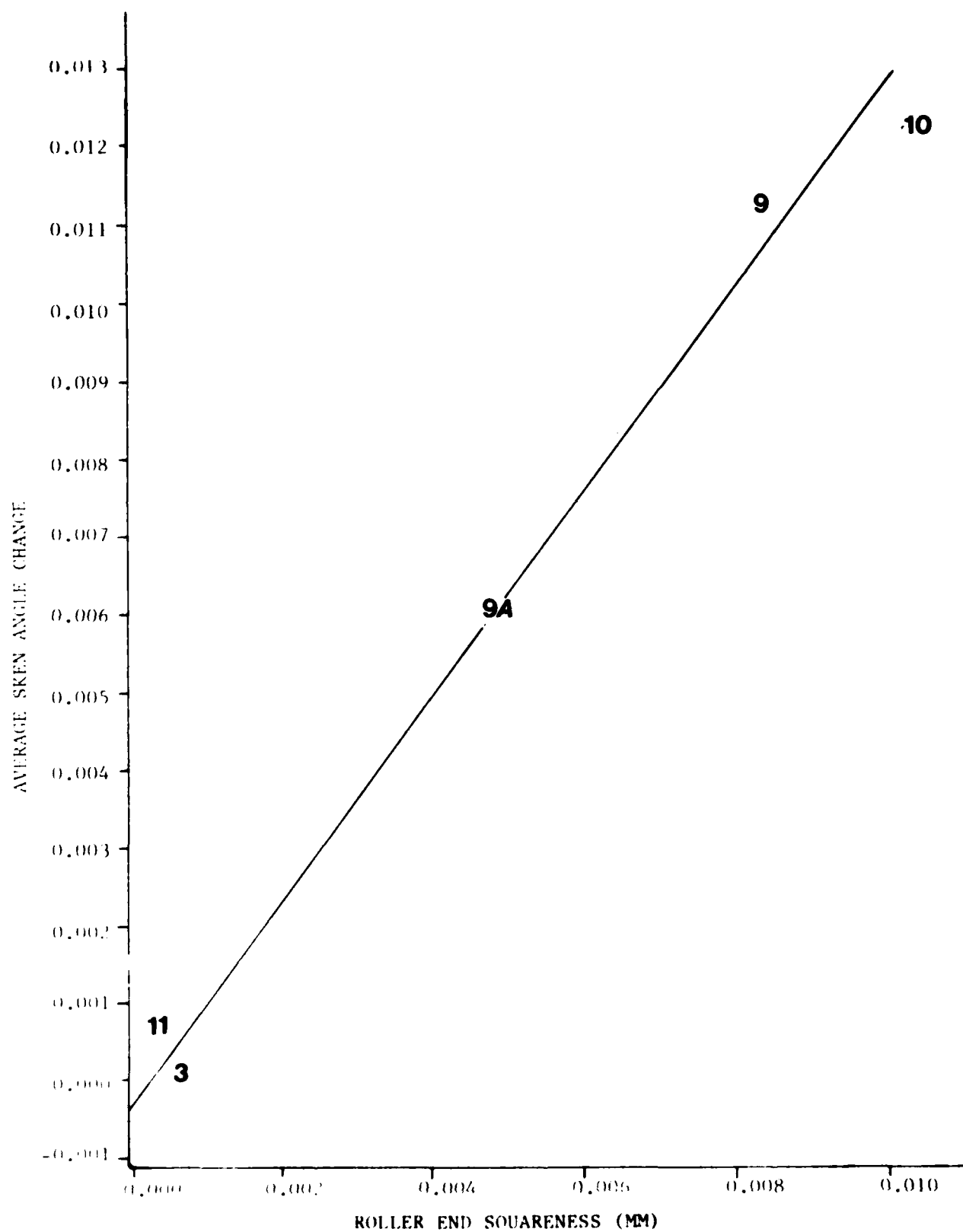**FIGURE 26**   **AVERAGE WEIGHT LOSS vs ROLLER END SQUARENESS**

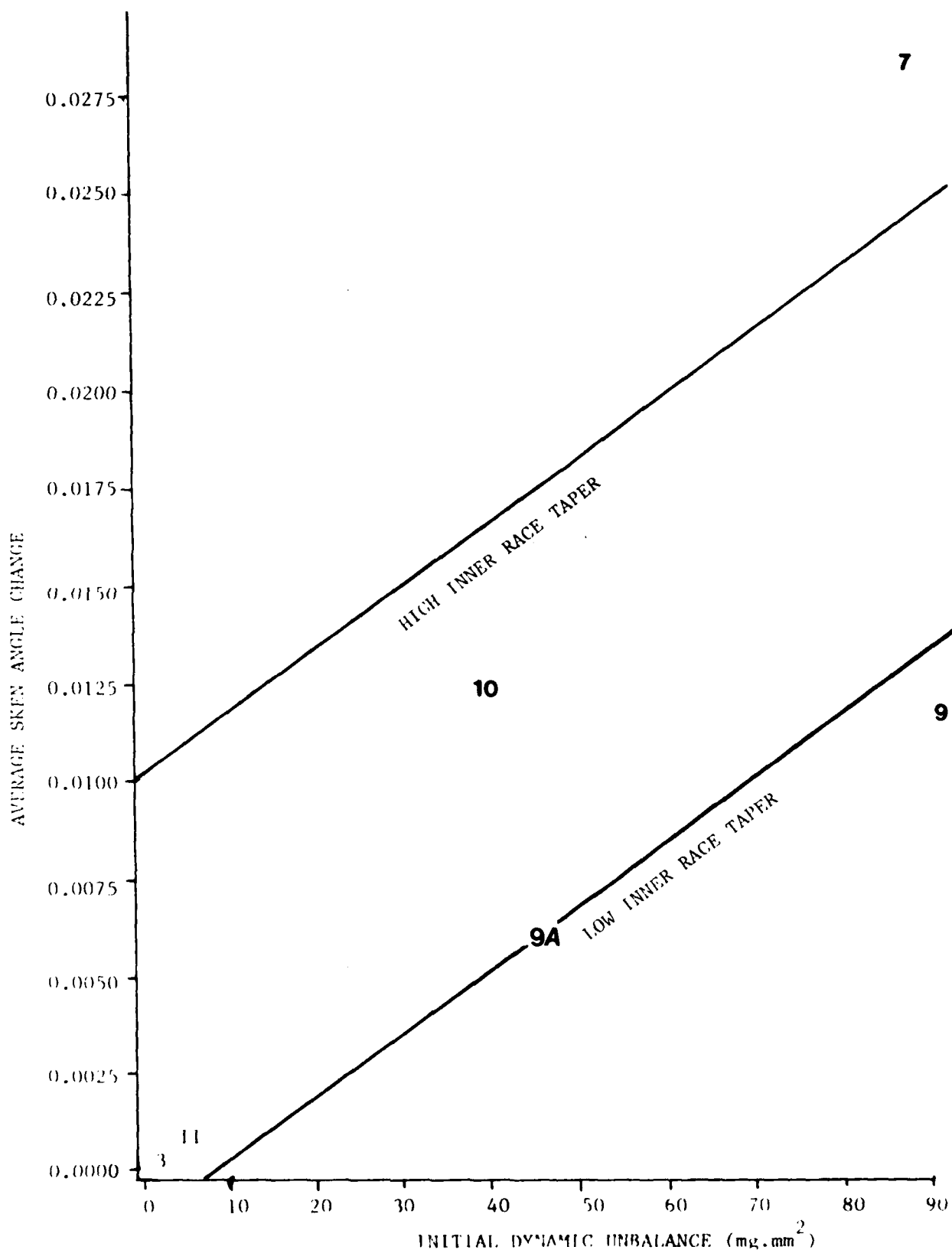FIGURE 27   AVERAGE SKEW ANGLE CHANGE
vs ROLLER END SQUARENESS

FIGURE 28 AVERAGE SKEW ANGLE CHANGE vs
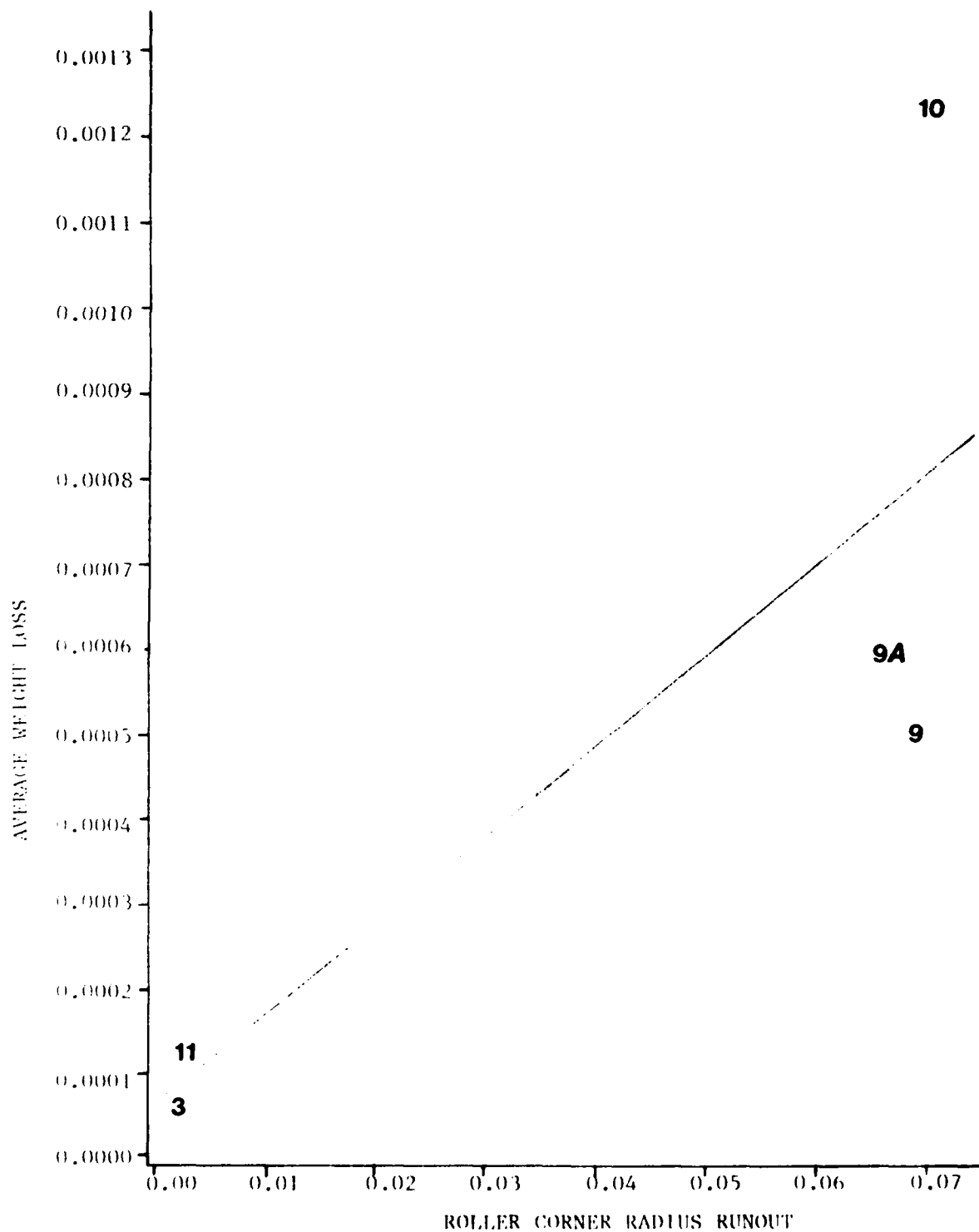INITIAL ROLLER DYNAMIC UNBALANCE
(AT HIGH AND LOW INNER RACE TAPER)

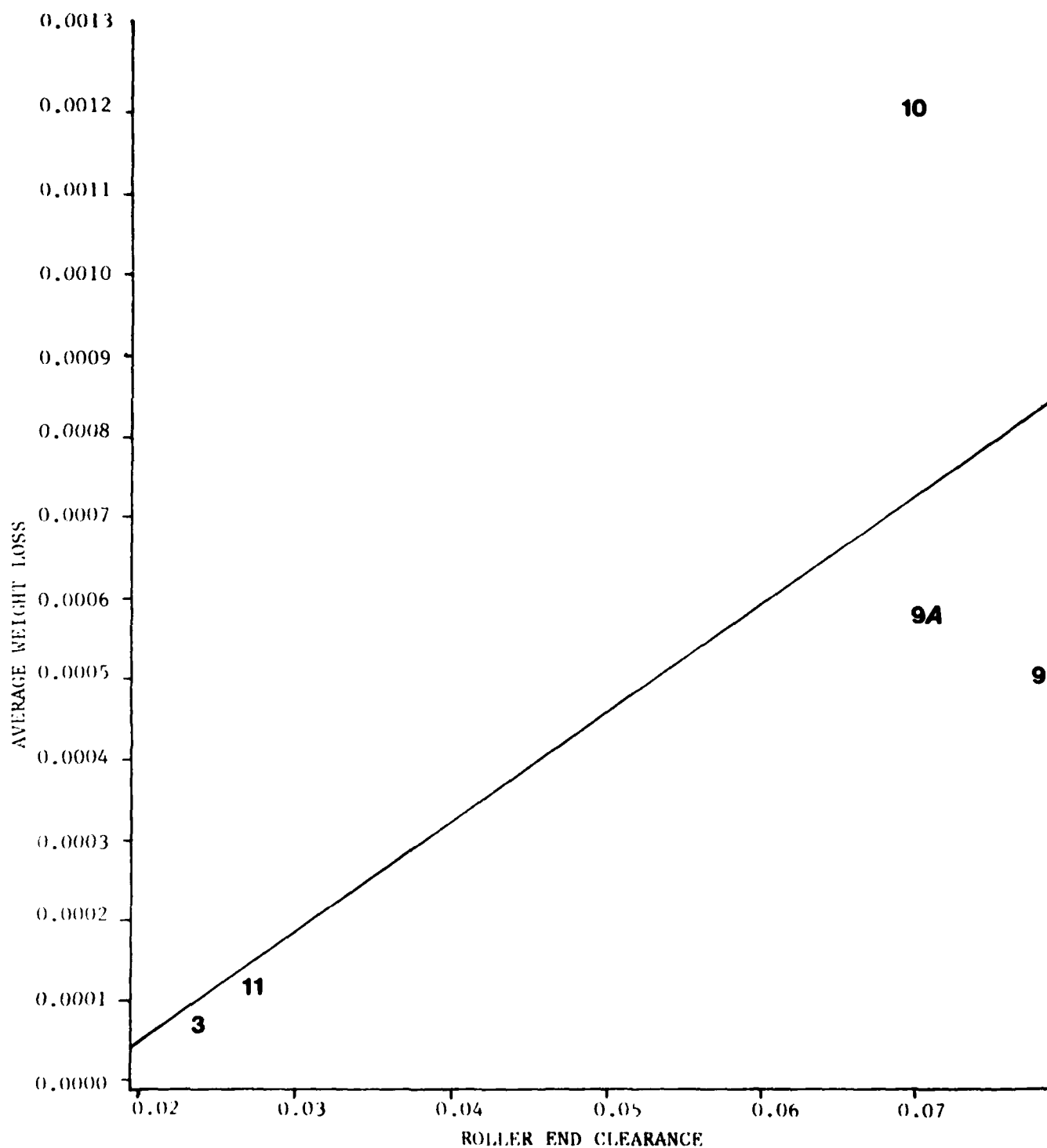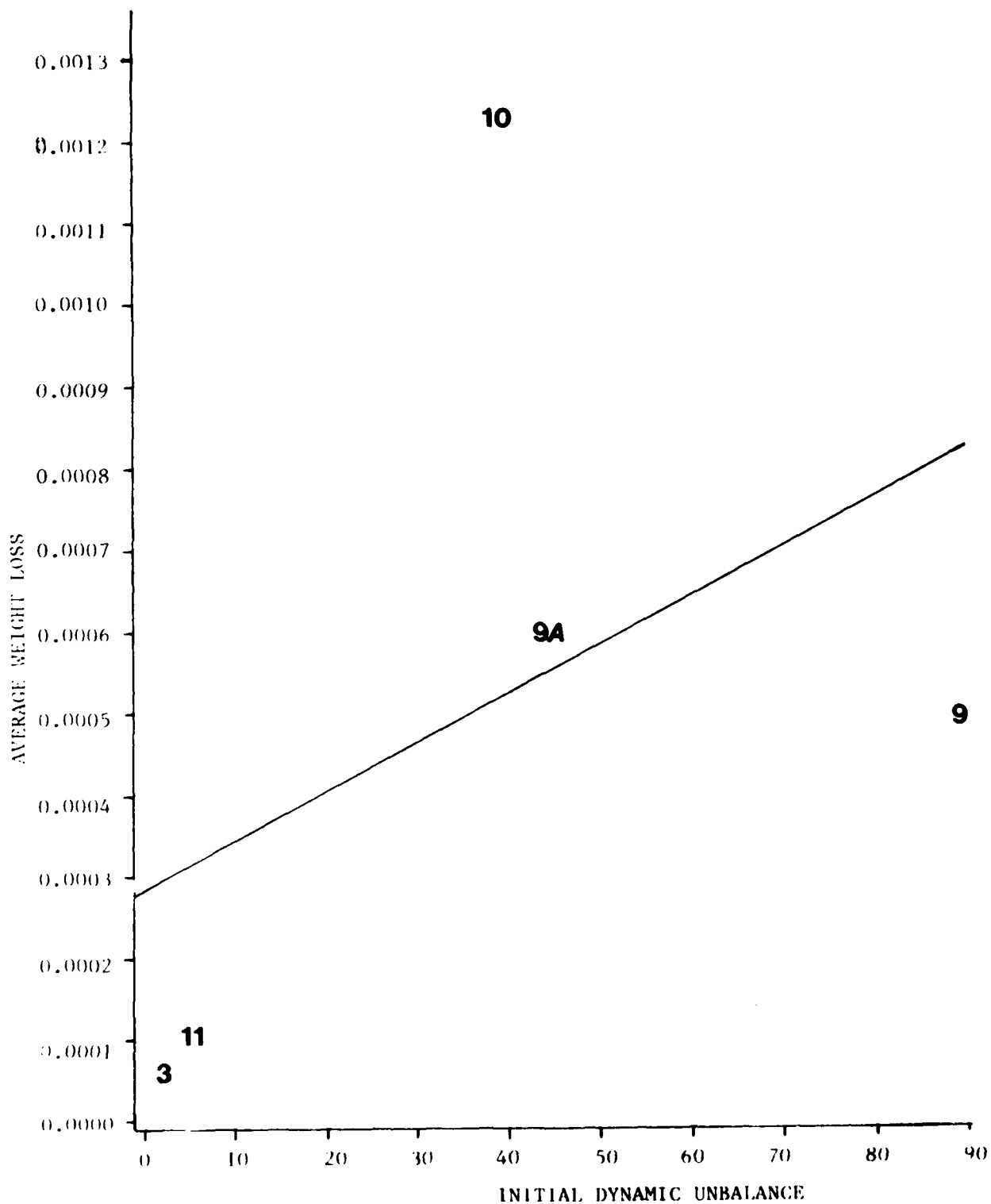FIGURE 29 AVERAGE WEIGHT LOSS vs ROLLER
CORNER RADIUS RUNOUT

FIGURE 30   AVERAGE WEIGHT LOSS vs ROLLER
              END CLEARANCE

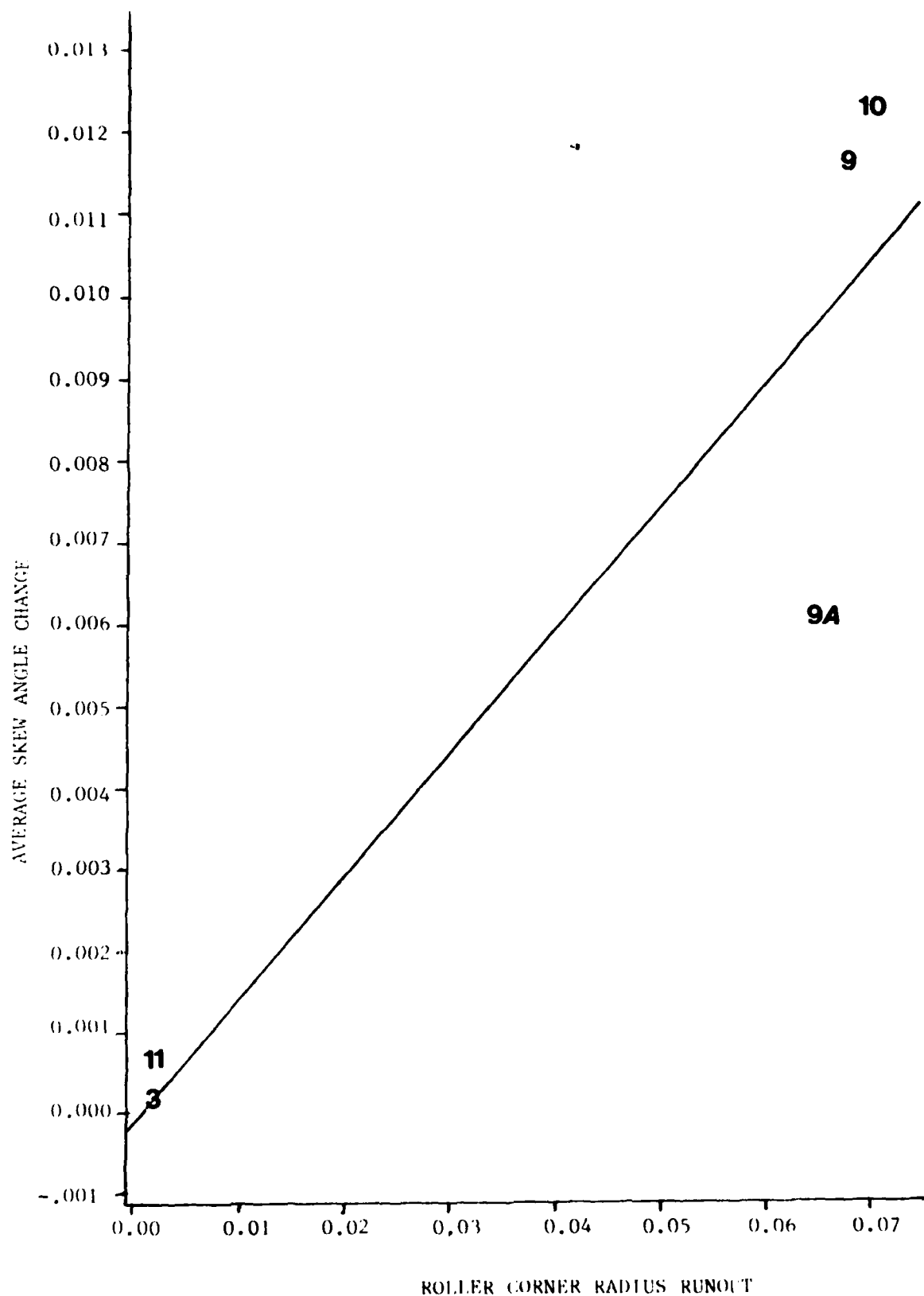FIGURE 31 AVERAGE WEIGHT LOSS vs INITIAL ROLLER DYNAMIC UNBALANCE
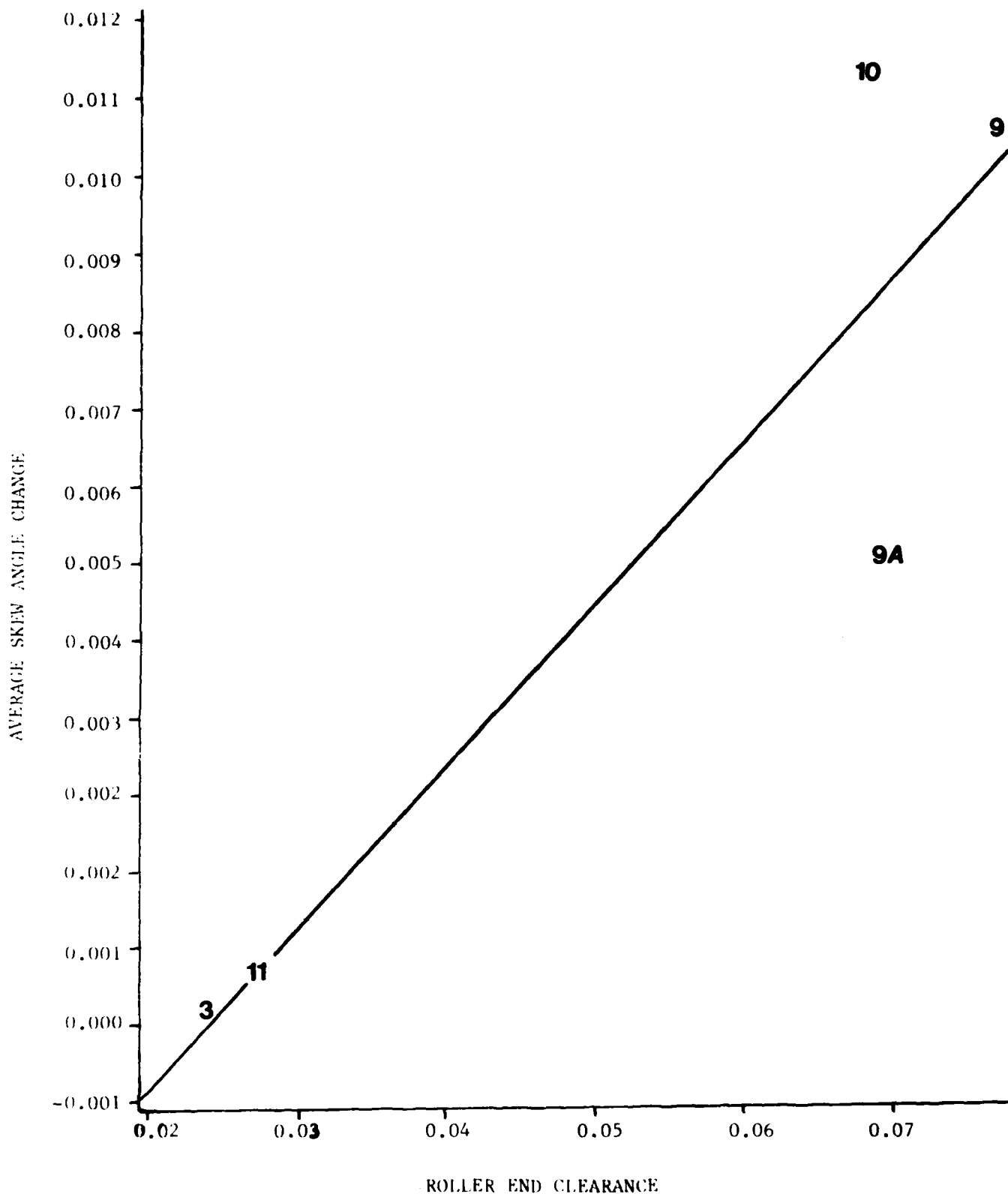
FIGURE 32   **AVERAGE SKEW ANGLE CHANGE vs ROLLER CORNER RADIUS RUNOUT**

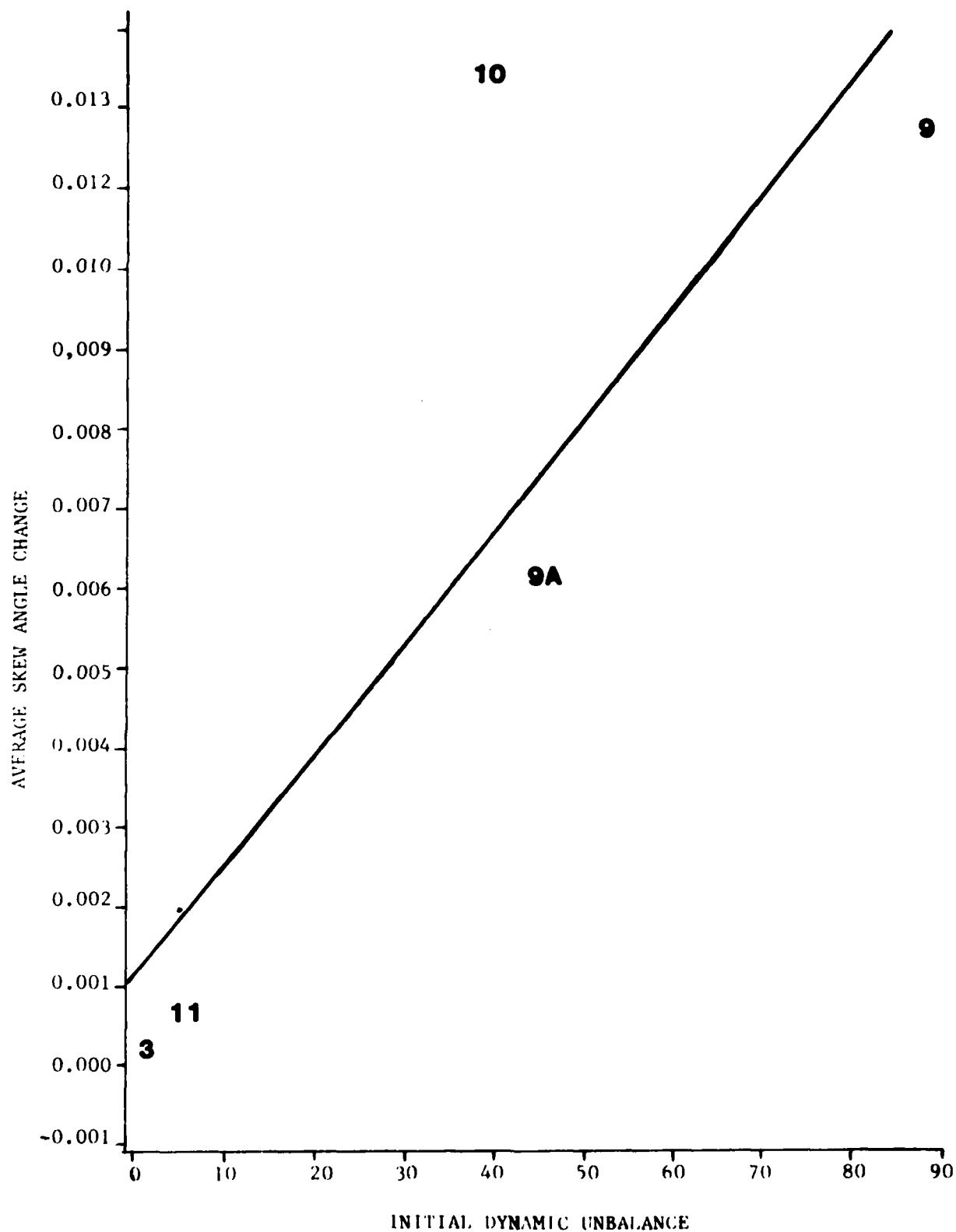**FIGURE 33** **AVERAGE SKEW ANGLE CHANGE vs ROLLER END CLEARANCE**

FIGURE 34   AVERAGE SKEW ANGLE CHANGE vs
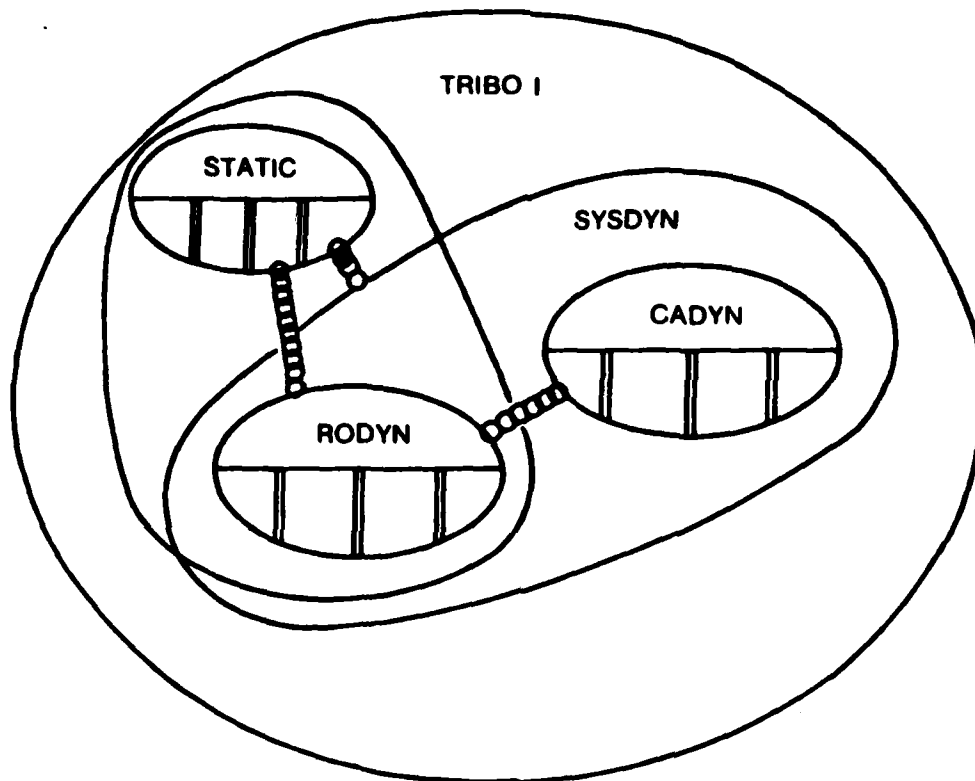INITIAL ROLLER DYNAMIC UNBALANCE

FIGURE 35   TRIBO 1   MODULAR PROGRAM CONSTRUCTION

5.0 CONCLUSIONS

The temperature measurements carried out on the bearing outer rings all show the expected trend of increasing temperature with dn number. The average ring temperature increase from 1.0 Mdn to 3.0 Mdn is generally in the range of 50°F to 150°F. The oil temperature rise in passing through the bearing generally falls within the range of 50°F to 75°F.

A survey of bearing cage speed versus the shaft speed indicates that at values below 2.6 Mdn, the cage speed is proportional to the loading as well as oil flow rates. At speeds above 2.7 Mdn, cage slip is minimal and at 3.0 Mdn, the cage speed is in the order of 97% of the epicyclic value and appears to be totally independent of applied load or oil flow rates.

The statistically useable data represents only 4 individual bearing designs out of the 14 contained in the original designed experiment. Statistical analysis of the data submitted led to the conclusion that the effects of at least four of the independent variables were confounded; that is, cannot be separated. It was further concluded that nothing was to be gained by using this data to attempt a modification of the existing TRIBO I wear model. The parametric trends already incorporated in TRIBO I based on earlier 124 mm bearing data are not contradicted by the limited 60 mm data. Based on these facts, no changes were made to the TRIBO I wear model as a result of the subject study.

References

1. Technical Report No. NAPC-PE-60C, "Development Of
    Mainshaft High Speed Cylindrical Roller Bearings For
    Gas Turbine Engines", Vol. I-IV, November 1980.

2. Technical Report No. AFWAL TR-80-2071, "High Speed
    Cylindrical Roller Bearing Development", August 1980.

3. Technical Report No. NAPC-PE-114C, "Bearing Roller
    Stability Model", May 1985.

END
DTIC
7_86